Small

NANO · MICRO small
www.small-journal.com

REVIEW OPEN ACCESS

Mesoporous Materials for Electrochemical Biosensors: From Broad Structure to Silica Film

Vinh Khanh Ho[1,2] | Tuan-Khoa Nguyen[1,2] | Sina Jamali[1,3] | Nam-Trung Nguyen[1,2]

[1]Queensland Quantum and Advanced Technologies Research Institute, Griffith University, Nathan, QLD, Australia | [2]School of Engineering and Built Environment (EBE), Griffith University, Nathan, QLD, Australia | [3]School of Environment and Science (ESC), Griffith University, Nathan, QLD, Australia

Correspondence: Sina Jamali (s.jamali@griffith.edu.au) | Nam-Trung Nguyen (nam-trung.nguyen@griffith.edu.au)

Received: 28 September 2025 | **Revised:** 7 January 2026 | **Accepted:** 12 January 2026

Keywords: anti-biofouling | electrochemical biosensor | gating effect | mesoporous materials | mesoporous silica | signal amplification

ABSTRACT

Mesoporous materials, characterized by tunable pore structures, large surface areas, and versatile surface properties, have become essential for advancing electrochemical biosensors. Their unique structural features enable efficient immobilization of biomolecules, enhancing electron transfer and amplifying signal transduction, which are vital for precise and selective detection of analytes within complex biological environments. This review provides a thorough discussion of scaffold-based mesoporous materials, including mesoporous silica, carbon, metals, metal oxides, metal-organic and covalent organic frameworks. We are focusing on their design strategies, synthesis techniques, and functional integration into biosensing systems. We emphasize recent innovations that leverage these materials for health monitoring and clinical diagnostics, targeting clinically relevant biomarkers such as glucose, nucleic acids, proteins, and metabolites linked to specific diseases. Moreover, we explore the role of mesoporous silica thin films in the operation of miniaturized biosensors, highlighting their potential in wearable and point-of-care applications. By systematically evaluating performance metrics and addressing reproducibility and scalability challenges, this review outlines crucial pathways for future research. Additionally, we discuss how advances in materials science, surface enhancement, and device integration are driving the development of next-generation real-time, non-invasive, and personalized diagnostic tools.

1 | Introduction

Diagnostics plays a critical role in both identifying diseases and guiding treatment. Early diagnostic measures are crucial for detecting diseases (preventive strategies) or for assessing the efficacy of treatment (prognostic evaluations). Numerous biodevices have been developed for the analysis of blood gases, glucose/lactate/cholesterol levels, nucleic acid sequences,

Abbreviations: 3DG@CNT, Three-dimensional graphene-carbon nanotubes; Ab, Antibody; AFM, Atomic force microscopy; Apt, Aptamer; APTES, (3-aminopropyl)triethoxysilane; APTMS, (3-aminopropyl)trimethoxysilane; bp-SNA, Bipolar silica nanochannel arrays; BSA, Bovine serum albumin; CA, Chronoamperometry; CA15-3, Cancer antigen 15-3; CA19-9, Cancer antigen 19-9; CC, Carbon cloth; Cdna, Complementary deoxyribonucleic acid; CE, Counter electrode; CEA, Carcinoembryonic antigen; CFME, Carbon fiber microelectrode; COF, Covalent organic frameworks; CTAB, Cetyltrimethylammonium bromide; cTnI, Cardiac troponin i; CV, Cyclic voltammetry; DNA, Deoxyribonucleic acid; DPV, Differential pulse voltammetry; EASA, Electrochemical assisted self-assembly; EC, Electrochemical; ECL, Electrochemiluminescence; EDC, N-ethyl-N′-(3-(dimethylamino)propyl)carbodiimide; EIS, Impedance spectroscopy; ELISA, Enzyme-linked immunosorbent assay; ErGO, Electrochemically reduced graphene oxide; FTIC, fluorescein 6-isothiocyanate (isomer II); FTO, Florine-doped tin oxide; GA, Glutaraldehyde; GCE, Glassy carbon electrode; GDH, Glucose dehydrogenase; HMSN, Hollow-type mesoporous silica; ITO, Indium tin oxide; LDH, Layered double hydroxides; LEGE, Laser engraved graphene electrode; LoD, Limit of detection; LSV, Linear sweep voltammetry; MB, Methylene blue; MCM, Mobil Composition of Matter; MIL, Materials of Institute Lavoisier; miRNA, Micro ribonucleic acid; MOF, Mesoporous metal-organic frameworks; MSF, Mesoporous silica film; MSN, Mesoporous silica nanoparticles; NHS, N-hydroxysuccinimide; NADH, 1,4-Dihydronicotinamide adenine dinucleotide; NMGE, Nanostructured mesoporous gold electrode; NPs, Nanoparticles; OMC, ordered mesoporous carbon; ORMOSIL, Organically modified silica; p-GCE, Pretreated-glassy carbon electrode; PMO, Periodic mesoporous organosilica; PSA, Prostate-specific antigen; QDs, Quantum dots; R_{ct}, Electron-transfer resistance; RE, Reference electrode; RNA, Ribonucleic acid; SARS-CoV-2 IgG, Severe acute respiratory syndrome coronavirus-2-immunoglobulin G antibody; SARS-CoV-2 RBD, Severe acute respiratory syndrome coronavirus-2-receptor binding domain; SBA, Santa Barbara amorphous; SEM, Scanning electron microscopy; SPCE, Screen-printed carbon electrode; SWV, Square wave voltammetry; TEM, Transmission electron microscopy; TEOS, Tetraethyl orthosilicate; UA, Uric acid; VMSF, Vertically-ordered mesoporous silica film; WE, Working electrode.

protein/peptide studies, toxicity, immunoassays, environmental monitoring, and forensic investigations [1–4]. A biosensor designed for monitoring blood glucose levels has been successfully commercialized [5]. Due to their portability and the expedited turnaround for results, biosensors are projected to address several unmet demands within the diagnostics industry [6–8].

Biosensors based on 3D nanomaterials have attracted significant attention in recent years, driven by the growing need to detect specific molecules present in the human body and its surrounding environment [8, 9]. Their architectures include interconnections between macro- and mesopores that inhibit aggregation and restacking. Therefore, these channels expose the inner surface and enable molecules and ions to access the void spaces. This feature has enabled significant advances in biosensors, including catalysis, drug delivery, and sensing [10]. The versatility of these materials stems from their structural properties and their ability to be functionalized, enabling tailored interactions with target molecules and enhancing their effectiveness across a range of biomedical and environmental applications. This adaptability is crucial for advancing technologies that optimize the performance of these materials and address complex challenges in medicine and environmental science [8].

Emerging scaffolding nanomaterials, characterized by low cytotoxicity, the capacity to stimulate cell proliferation, and versatile fabrication methods, have garnered significant attention in biomedical science. Various modifications, including the application of surface functionalities, surface charge modification (either negative or positive) and hydrophobic character, as well as the controlled flexibility or rigidity, can be applied to the scaffold materials to modulate their physicochemical properties and biological conformity. These materials have been utilised for the detection of analytes such as cancer biomarkers [11, 12], foodborne pathogens [13, 14], dopamine [15], uric acid [16, 17], ascorbic acid [18, 19], glucose [20, 21], cortisol [22], and hydrogen peroxide [23–25].

The synthesis, properties, and broad applications of mesoporous materials, including silica, carbon, and metals, in areas such as drug delivery and sensing have already been well documented [26–29]. Published reviews have highlighted the functional role of oriented mesoporous silica in (bio)sensing and as a molecular sieve [30–32]. In this review, we first examine mesoporous materials as platforms for sensing and the detailed discourse surrounding biosensor applications, with an emphasis on recent contributions. We highlight new developments, such as the gating effect enabled by vertically ordered mesoporous silica, functionalized with antibodies and aptamers. Such works create unprecedented opportunities through advanced mesoporous silica structures in analytical electrochemical biosensors and the translation into a wearable device. A variety of detection methods have been employed to identify distinct biomarkers. This review delineates the analytical efficacy of each technique, providing a comparative analysis for the optimal detection of various analytes. Additionally, the underlying mechanisms governing each method are discussed. This comprehensive examination not only highlights the strengths and limitations of current detection methods but also emphasizes the need for innovative approaches to enhance sensitivity and specificity, as well as the potential of these methods as biosensing materials for wearable health monitoring applications.

2 | Fundamentals of Electrochemical Biosensor

An electrochemical biosensor is a specialized analytical tool that translates a chemical signal from a specific reaction or molecular recognition event into a quantifiable electrical signal. The electric signal, such as current, potential, or impedance, correlates with the concentration of the target analyte [33]. These devices are fundamentally electrochemical cells that comprise four key components: a working electrode (WE), a reference electrode (RE), a counter electrode (CE), and an electrolyte [34, 35]. The WE serves as the primary sensing interface. The surface of the WE is frequently modified with catalysts or recognition elements to impart selectivity and sensitivity. The RE, commonly a silver/silver chloride (Ag/AgCl) system, establishes a stable, non-polarizable potential benchmark against which the WE potential is measured. The CE, or auxiliary electrode, is fabricated from an inert material (e.g., platinum or graphite) and serves to complete the electrical circuit by passing current, predominantly in amperometric and impedimetric type sensors. These components are immersed in an electrolyte, an ionically conductive medium that facilitates ion transport to maintain overall charge neutrality [36]. Based on the signal transduction mechanism, these devices are classified as potentiometric, impedimetric, photoelectrochemical, electrochemiluminescent, or most commonly, voltametric/amperometric sensors. The voltammetric/amperometric category utilizes a variety of interrogation strategies, differentiated by the applied potential waveform, including cyclic voltammetry (CV), chronoamperometry (CA), linear sweep voltammetry (LSV), differential pulse voltammetry (DPV), and square wave voltammetry (SWV) [33].

Mesoporous materials in electrochemical sensors typically do not serve as the transducer themselves but rather function as high-performance modification layers to enhance their sensing capabilities (Figure 1). Depending on their intrinsic electrical properties, mesoporous materials exert two distinct effects on the transducer. **Insulating materials**, such as mesoporous silica, are electrically nonconductive and primarily serve as structural and passivation layers. These materials provide a large specific surface area for biomolecule immobilization, acting as selective barriers to minimize interference and shield the recognition element from denaturation. In these systems, electron transfer occurs predominantly at the underlying electrode surface beneath the silica layer [7, 37]. In contrast, **conductive materials**, including mesoporous carbons, metals, and modified silica, act as 3D extensions of the electrode. These materials combine high surface area, ordered porosity and high electrical conductivity, thereby participating directly in signal transduction. The conductive mesoporous framework forms an interconnected scaffold that reduces electron transport distance, facilitating faster charge transfer, and amplifying the overall electrochemical response [38, 39].

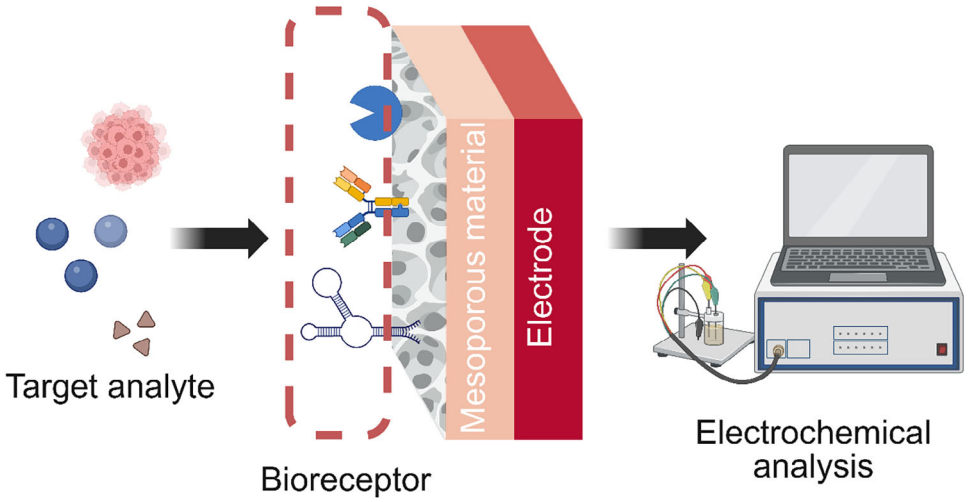

FIGURE 1 | Working mechanism of an electrochemical biosensor [33].

3 | Overview of Mesoporous Materials for Electrochemical Biosensors

Porous materials are classified by pore size according to the International Union of Pure and Applied Chemistry: microporous, mesoporous, and macroporous. Mesoporous materials are a unique class of porous solids structured by well-defined pores with diameters in the range of 2–50 nm. In contrast, microporous materials refer to materials with pore sizes less than 2 nm, while macroporous materials exhibit pore diameters larger than 50 nm [40]. The intermediate regime provides an advantageous balance: large enough to facilitate rapid mas transport of electrolytes and biomolecules, yet small enough to maintain high surface area [29, 41, 42]. These features distinguish mesoporous materials as highly attractive for electrochemical biosensing, where signal amplification, efficient charge transfer, and selective biomolecule immobilization are crucial [38, 43–45]. In the following subsections, we discuss five main classes of mesoporous materials that have been most widely explored in this context. These include silica and non-silica materials spanning mesoporous carbon, mesoporous metals and metal alloys, mesoporous metal oxides, mesoporous metal-organic frameworks and covalent organic frameworks.

3.1 | Mesoporous Silica

Mesoporous silica nanoparticles (MSNs) have received considerable attention in recent decades owing to their ease of synthesis, low toxicity, high chemical stability, cost-effectiveness, and highly controlled mesoporous size and shape [7]. MSNs have been synthesised with various morphologies (Figure 2), such as molecular sieves (MCM-41, MCM-48, and MCM-50) [46–50], Santa Barbara Amorphous (SBA) [51], hollow-type mesoporous silica (HMSN) [52], periodic mesoporous organosilica (PMO) [53], core-mesoporous silica shell structures and organically modified silica (ORMOSIL) nanoparticles [54, 55].

Ordered silica-based mesoporous materials consist of a periodic and regular arrangement of well-defined mesopores and an amorphous inorganic framework structure. These materials are known for their unique properties, specifically, high porosity (pore volume > 0.7 mL/g), with high specific surface areas (500–1500 m^2/g), and represent characteristics of both silica gels and molecular sieve zeolites [7, 41, 56–60]. Ordered mesoporous silicas usually can be obtained by the sol-gel process, which will be discussed in the next section, involving the hydrolysis and condensation of tetraalkoxysilane $Si(OR)_4$ as the precursor of silica source, in the presence of a supramolecular template such as surfactants (micelles).

MSNs are widely utilised as carrier materials in a variety of controlled-release technologies due to their large specific surface area, excellent biocompatibility, and substantial drug-loading capacity [40, 61–63]. Exploiting these properties, Jimenez-Falcao et al. developed an electrochemical aptasensor using MSNs loaded with methylene blue as the redox probe, thereby augmenting the signal of these biosensors by capping with an avidin/imminobiotin pH-responsive gate-like ensemble [64]. This aptasensor, designed for the detection of carcinoembryonic antigen, was formed by conjugating a biotinylated, thiol-functionalized anti-carcinoembryonic antigen DNA hairpin aptamer to gold nanoparticles modified screen-printed carbon electrodes. The biosensing method relies on the unique unfolding of the aptamer upon CEA binding. The process exposes the biotin moiety and facilitates binding to avidin-functionalized MSNs. This project demonstrated the feasibility of customizing the design of similar nanocarriers with controlled loading capacity and size, and of utilising various redox probes as cargo, presenting new opportunities for the development of highly sensitive electrochemical biosensors [64]. Li et al. implemented a similar approach. The team developed an innovative split-type electrochemical immunosensor that employs a controlled-release strategy for sensitive detection of the tumor marker CA19-9 [65]. In this approach, glucose is encapsulated within MSNs and sealed with functionalized zinc sulphide (ZnS) to create a signal-amplifying complex. By separating the immune recognition process from electrochemical analysis, the authors claim that the immunosensor effectively addresses the challenge of low detection sensitivity caused by biofouling (Figure 3A). The sensor exhibits a wide linear detection range (0.001–100 U/mL) with an impressive detection limit of 0.5 mU/mL, demonstrating its

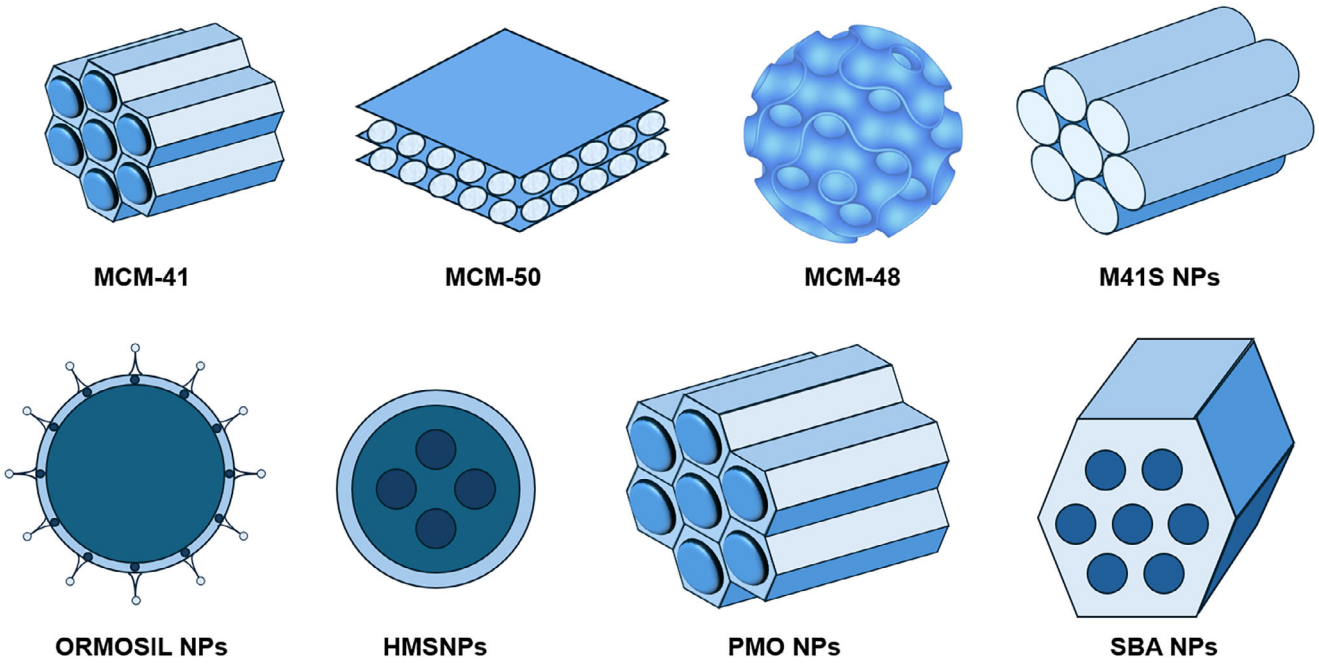

FIGURE 2 | Typical morphologies of MSNs: molecular sieves (MCM-41, MCM-48, and MCM-50), Santa Barbara Amorphous (SBA), hollow-type mesoporous silica (HMSN), periodic mesoporous organosilica (PMO), organically modified silica (ORMOSIL) nanoparticles [46].

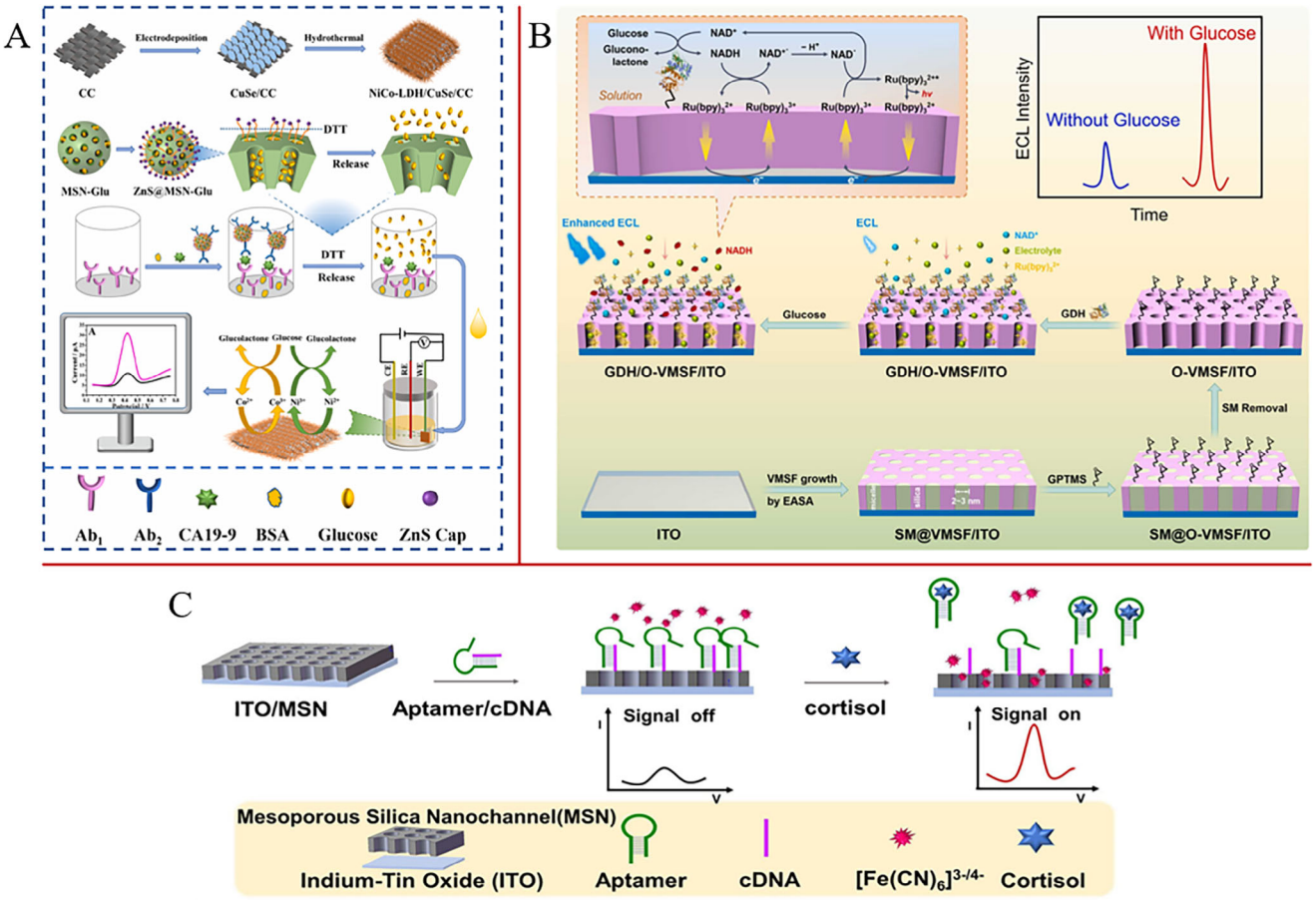

FIGURE 3 | Mesoporous silica-based electrochemical sensors. (A) Fabrication process of the sandwich sensor and signal amplification mechanism for the detection of carbohydrate antigen 19-9 (CA19-9). Reproduced with permission [65]. Copyright 2023, Elsevier. (B) Schematic of preparation of GDH/O-VMSF/ITO electrode and the electrochemiluminescence enzyme biosensor for detecting glucose. Reproduced with permission [21]. Copyright 2024, Elsevier. (C) Functionalized VMSF role in the signal conversion interface of the working for detecting cortisol. Reproduced with permission [22]. Copyright 2024, American Chemical Society.

high sensitivity [65]. While the design shows promise for highly sensitive detection of the tumor marker in PBS, further research in relevant biological media is necessary to evaluate the impacts of biofouling agents and the practical real-world considerations of the design.

Mesoporous silica films (MSFs) have attracted attention as promising structures for electrochemical biosensors [30, 66–68]. Their appeal lies in the well-ordered pore arrangement, consistent pore size of 2 – 3 nm, and ease of functionalization. MSFs enhance diffusion through their nanochannels, thereby improving the sensitivity of biomolecule detection. Huang et al. introduced a "signal-on" electrochemiluminescence (ECL) enzyme biosensor to detect glucose in human serum and artificial sweat (Figure 3B) [21]. This ECL enzyme biosensor was constructed by immobilizing a glucose dehydrogenase (GDH) monolayer on the external surface of a vertically ordered mesoporous silica film (VMSF), thereby facilitating the diffusion of $Ru(bpy)_3^{2+}$ through the silica nanochannels. The NAD^+-active GDH layer catalyzes the oxidation of glucose substrates, producing NADH in the process. The ECL intensity directly correlates with glucose concentration, enabling quantitative analysis of glucose levels. The biosensor demonstrated a wide linear detection range for glucose (10 nM to 1 mM) and a low limit of detection (1.5 nM) in diluted samples [21]. Luan et al. developed a wearable electrochemical biosensor for cortisol detection in sweat, a small-molecule hormone widely recognized as a key stress indicator (Figure 3C) [22]. The team employed aptamer/cDNA hybrids to modify the surface of MSN as the recognition element. This modified structure served as a gating mechanism, in which binding of the analyte to the aptamer triggered aptamer unfolding and detachment, thereby opening the gate, as illustrated in Figure 3C [22]. However, the irreversible release of aptamer/cDNA hybrids limited device reusability, highlighting the need for optimized aptamer selection or regenerative strategies to improve this concept.

3.2 | Other Mesoporous Materials

3.2.1 | Mesoporous Carbon

Traditional porous carbon materials possess a rich historical background and have been effectively utilised across a variety of applications. They serve as adsorbents for contaminants, in filtration processes, for energy storage and solutions, and as supporting matrices for electrocatalysts [26, 38, 69, 70]. Electrodes modified with mesoporous carbon demonstrate a substantial electroactive surface area and display efficient charge transfer mechanisms. Moreover, the characteristics of the mesoporous carbon matrix include uniformity and similarity to graphite-like domains and stacking heights, a reduced surface functional group content, and a minimal frequency of defects such as twists, non-aromatic connections, and carbon valencies [71]. Collectively, these compelling structural attributes, along with densely concentrated edge plane defect sites, facilitate the immobilization of biomolecules, proteins, and enzymes without the need for linkers [72, 73].

Furthermore, porous carbon consists solely of carbon elements, which may improve compatibility with bioreceptors and potentially extend shelf life. These comprehensive features have propelled the use of mesoporous carbon as a promising material for developing electrochemical biosensing platforms [45, 73–76]. For example, Zhong et al. engineered an enzyme-modified electrode for an electrochemical biosensor. The complex enzyme consists of a mesoporous carbon/zirconium-based metal-organic framework composite integrated with laccase for detection of tetracycline [73].

Jain et al. proposed a novel nanostructured mesoporous carbon-based electrochemical biosensor specifically for the detection of swine influenza [77]. These modified electrodes facilitated fast charge-transfer processes due to their favourable electronic properties with a mean pore size of 4.8 nm [77]. Moreover, because porous carbon was composed solely of carbon, it offered high biocompatibility with bioreceptors and demonstrated excellent long-term stability. Collectively, these unique structural and electronic properties made mesoporous carbon a promising material for the development of advanced electrochemical biosensors [77].

Wang et al. synthesised CdZnSeS quantum dots (QDs) amalgamated with ordered mesoporous carbon (OMC) and subsequently immobilized these onto a glassy carbon electrode surface for the detection of hydrogen peroxide [74]. The integration of QDs with the highly conductive mesoporous carbon structures markedly enhanced both the electrochemical performance and the electrochemical luminescence signal. Their findings indicated that the developed biosensor exhibited a higher electron transfer rate, a lower detection limit, greater selectivity, and greater stability than a glassy carbon electrode [74]. Leveraging the high surface area of mesoporous carbon to enhance binding, mobility, and collision probability, Wahab et al. fabricated well-dispersed superparamagnetic iron oxide nanoparticles on a mesoporous carbon support (Figure 4) [78]. As a proof-of-concept, the team developed a glucose assay with a limit of detection (LoD) of 2 μM in spiked samples. These findings demonstrate that homogeneously dispersed iron oxide nanoparticles on mesoporous carbon have potential as next-generation nanozymes for highly sensitive bioassays [78]. However, the limitation of this work lies in the fabrication of the materials needed to achieve the desired composite. It highlights that further research should focus on utilising the methodology of synthesizing the composite materials while maintaining their potential for sensitive bioassays.

3.2.2 | Mesoporous Metals and Metal Alloys

Mesoporous metals, distinguished by their nanoscale crystalline architectures and mesopores ranging from 2 to 50 nm, are classified as second-generation mesoporous materials due to their exceptional porosity, high surface areas, and enhanced electroconductive properties. These characteristics are the main reasons for their use in applications such as catalysis, electrocatalysis, and biosensing. Within catalytic systems, mesoporous metals enhance performance by augmenting activity, stability, and selectivity [79–83]. Mesoporous metals have garnered significant attention due to their unique physicochemical characteristics. Their high electrical and thermal conductivity enables a variety of applications in electrocatalysis, biosensing, and bioimaging [84–86]. Mesoporous gold films have recently attracted interest

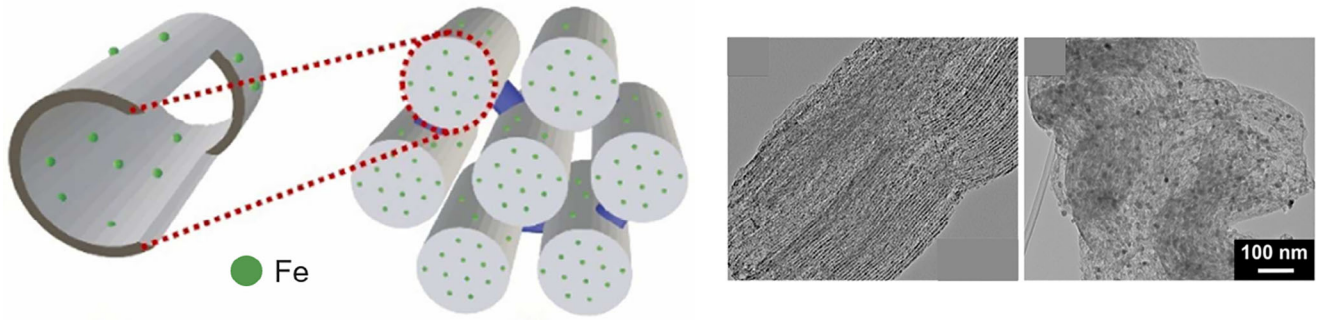

FIGURE 4 | Schematic representation of the iron oxide–mediated mesoporous carbon and SEM images of the modified mesoporous carbon. Reproduced with permission [78]. Copyright 2022, Elsevier.

for biosensor development due to their tunable pore size, high surface-to-volume ratio, surface roughness, and inherent electrochemical properties, which enable the development of low-cost, sensitive, and portable diagnostic devices [87–90].

Unlike bulk gold electrodes, mesoporous gold provides a vastly enlarged electroactive surface area, which facilitates greater biomolecule loading and more efficient electron transfer, thereby markedly enhancing the electrochemical signal. Ahmed et al. fabricated a biosensor based on a nanostructured mesoporous gold electrode for highly sensitive detection of protein phosphorylation with electrochemical signal amplification (Figure 5A) [87]. The appropriate pore size plays a pivotal role in biosensor design, balancing surface area and mass transport to ensure efficient immobilization of bioreceptors while maintaining rapid charge transfer for highly sensitive detection. Ahmed et al. fabricated an immune checkpoint protein analyzer chip for lung cancer via an electrochemical deposition of gold (III), with a controllable pore size [88]. As detailed in Figure 5B, atomic force microscopy (AFM) clearly revealed the matrix of these mesoporous gold films. The film with 18.3 nm pore size exhibited the highest sensitivity and efficiency for capturing targeted cancer cells, attributed to its homogeneous pore-size distribution across the surface, which provides a uniform nanoscale topography that maximizes surface contact with cell membranes and facilitates consistent biomolecule immobilization [88].

Leveraging the electrocatalytic activity and signal-amplification capabilities of the mesoporous gold electrode, an ultrasensitive and specific electrochemical sensor was engineered for the detection of miRNA (Figures 5C and 6). This constitutes a single-step assay capable of detecting a broad range of targets, achieving an ultra-low limit of detection at attomolar concentrations (Figure 5C) introduced by Masud et al. [89]. These works demonstrate significant translational potential for advancing high-performance diagnostic tools in clinical settings [89, 90].

Mesoporous metal alloy structures integrate the inherent catalytic properties of their constituent metals with the distinctive properties of mesoporous structures, thereby facilitating unique signal transduction and catalytic behaviors. Mesoporous alloy films composed of different metals exhibit diverse reactivities and standard redox potential (E°). These materials offer numerous benefits in electrocatalysis. In contrast to conventional nonporous noble metal-based electrocatalysts, mesoporous metal alloy nanoarchitectures incorporate multiple noble metals and thus considerably enhance electrocatalytic performance. The improvement is due to their ability to create a more advantageous electrical architecture, reducing the costs of electrode fabrication while preserving a high surface area and superior mass-transport characteristics. These features ultimately improve reaction kinetics and efficiency across a spectrum of electrochemical applications [91–98]. The tailored electrocatalytic properties form a favourable platform for electrochemical biosensing.

A good example of metal alloy structures is the as-synthesised mesoporous Au–Cu films, which exhibit vertically aligned mesopores and a uniform atomic distribution of Au and Cu over the entire film (Figure 7A) [98]. As a result, mesoporous Au–Cu films provide a large surface area with highly accessible pores for guest species, leading to higher performance in nonenzymatic glucose sensing than individual Au- or Cu-based nonenzymatic glucose sensors. Such vertically oriented tubular mesochannels can also be obtained using different alloy compositions such as Au–Ni [99].

Mesoporous metallic alloys have been successfully used for ultrasensitive nucleic acid detection, such as microRNAs (miRNAs), owing to their excellent catalytic activity [95, 100, 101]. miRNA, a small non-coding RNA (21–24 nucleotides) that controls over 30% of the human genome, is involved extensively in almost every cellular process, including cell differentiation, gene expression, and biological development [89, 95, 100, 101]. Building on the superparamagnetism of cobalt and iron together with the biocompatibility of gold, Kang et al. synthesised a magnetic mesoporous CoFeB amorphous alloy with tunable Co/Fe ratios via wet-chemical reduction and subsequently doped it with gold nanoparticles [100]. The resulting Au–CoFeB demonstrated high magnetization, large open mesopores (~12.5 nm) (Figure 7B), and excellent antibody accessibility. As a proof-of-concept, the material served as a dispersible nanovehicle in a sandwich-type electrochemical assay for the ultra-sensitive detection of p53 autoantibody in plasma, achieving a detection limit of 6 mU/mL [100] Park et al. studied a sensing platform for miRNA detection without amplification using mesoporous gold-silver alloy films (Figure 7C) [95]. The gold-silver alloy film was fabricated via electrochemical micelle assembly, using a block copolymer as a soft template that dictated pore formation and morphology. The films exhibit high electrocatalytic activity, enabling sensitive miRNA detection using differential pulse voltammetry [95]. Li et al. synthesised mesoporous

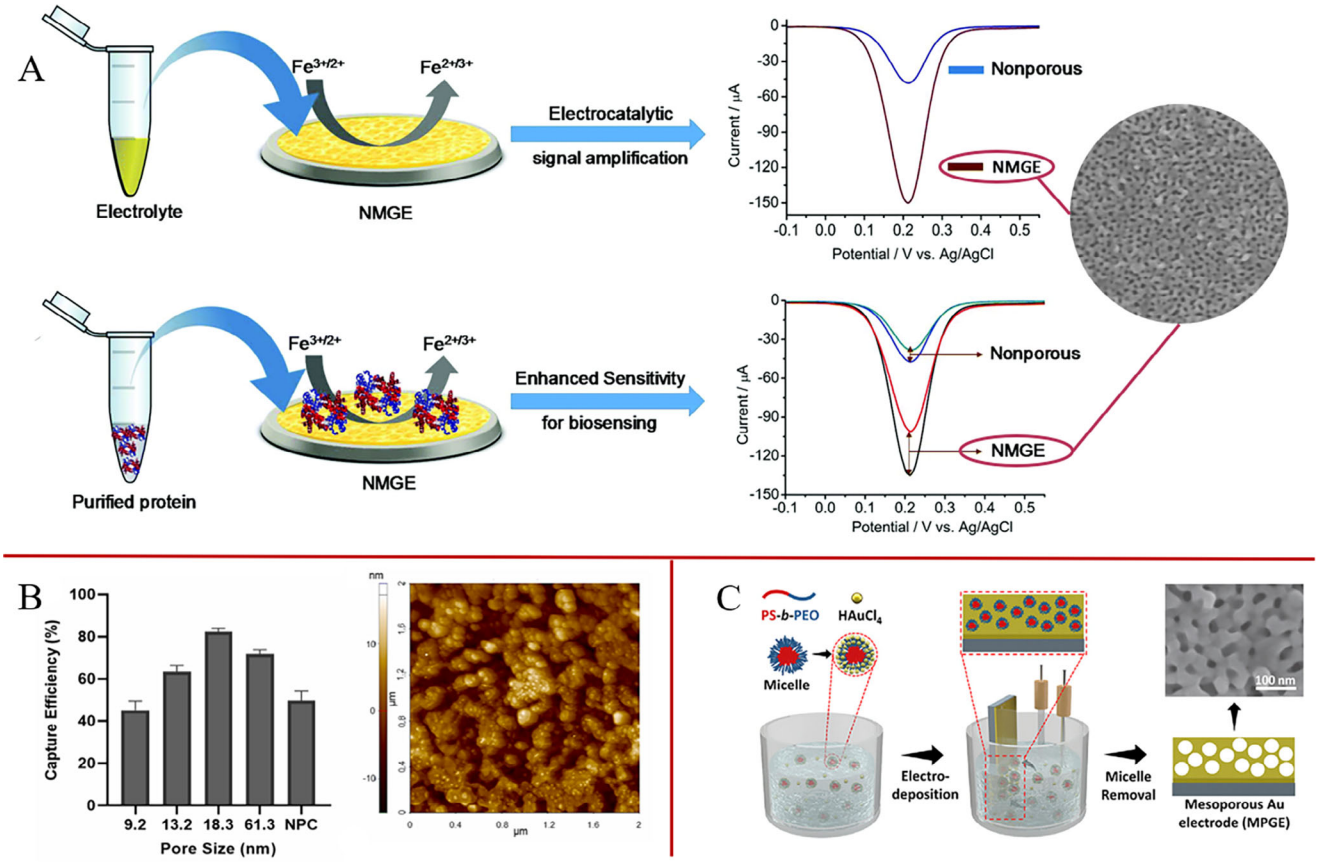

FIGURE 5 | (A) Schematic illustration of nanostructured mesoporous gold electrode (NMGE) for enhanced detection of protein phosphorylation via electrochemical signal amplification. Reproduced with permission [87]. Copyright 2020, Royal Society of Chemistry. (B) Schematic illustration of film characterization through SEM and AFM image. Reproduced with permission [88]. Copyright 2024, Elsevier. (C) Schematic illustration of the synthesis of mesoporous gold electrode through the electrodeposition process involving gold (III)-infused polymeric (block) micelles. The target miR-9-2 was conjugated onto the electrode via RNA-gold affinity (involving both conventional physisorption and chemisorption mechanisms). Reproduced with permission [89]. Copyright 2020, Elsevier.

trimetallic PdPtCu nanospheres (m-PdPtCu) with a well-defined morphology (Figure 7D) [101]. These mesoporous trimetallic nanospheres were first employed as a signal amplification strategy in a highly sensitive and selective immunosensor for the detection of trace amounts of prostate-specific antigen in human serum [101].

3.2.3 | Mesoporous Metal Oxides

After more than 30 years of intensive exploration and development, the field of mesoporous material synthesis has established a comprehensive system of methodologies centered on silica- and carbon-based materials, enabling precise control over critical properties such as thickness, aspect ratio, pore structure, and morphology [102–112]. However, due to the inherent properties of metal oxide materials, synthesis strategies that are effective in silica-based and carbon-based systems cannot be directly applied to metal oxides. For instance, the commonly rapid hydrolysis rate of metal oxide precursors makes it challenging to control the nucleation and growth process of materials. Also, the tendency for spontaneous crystallization hinders pore formation in the material, making the synthesis of mesoporous metal oxide materials extremely challenging.

Mesoporous transition metal oxides are an emerging class of porous materials due to their confined d-electrons, enhanced reactive surface-active sites, and interconnected pore structure. Mesoporous metal oxides have become a viable solution in many fields, including catalysis, sensing, energy storage, and conversion, due to their unique compositional and structural diversity. A range of metal oxides, such as iron and titanium oxides, has been examined as possible electrode materials for supercapacitors due to their mesoporous nature, which provides a large surface area and tunable pore size [113–115]. However, the practical application of metal oxides in electrochemical biosensors is significantly constrained by their inherent pH sensitivity. Future research should prioritize the development of mesoporous metal oxides that can operate across a broader pH range. This advancement is crucial for unlocking the next generation of materials suitable for reliable analysis in complex clinical samples, such as blood, saliva, and urine.

3.2.4 | Mesoporous Metal-Organic Frameworks and Covalent Organic Frameworks

Metal-organic frameworks (MOFs), also known as crystalline porous coordination polymers, are constructed from metal ions or

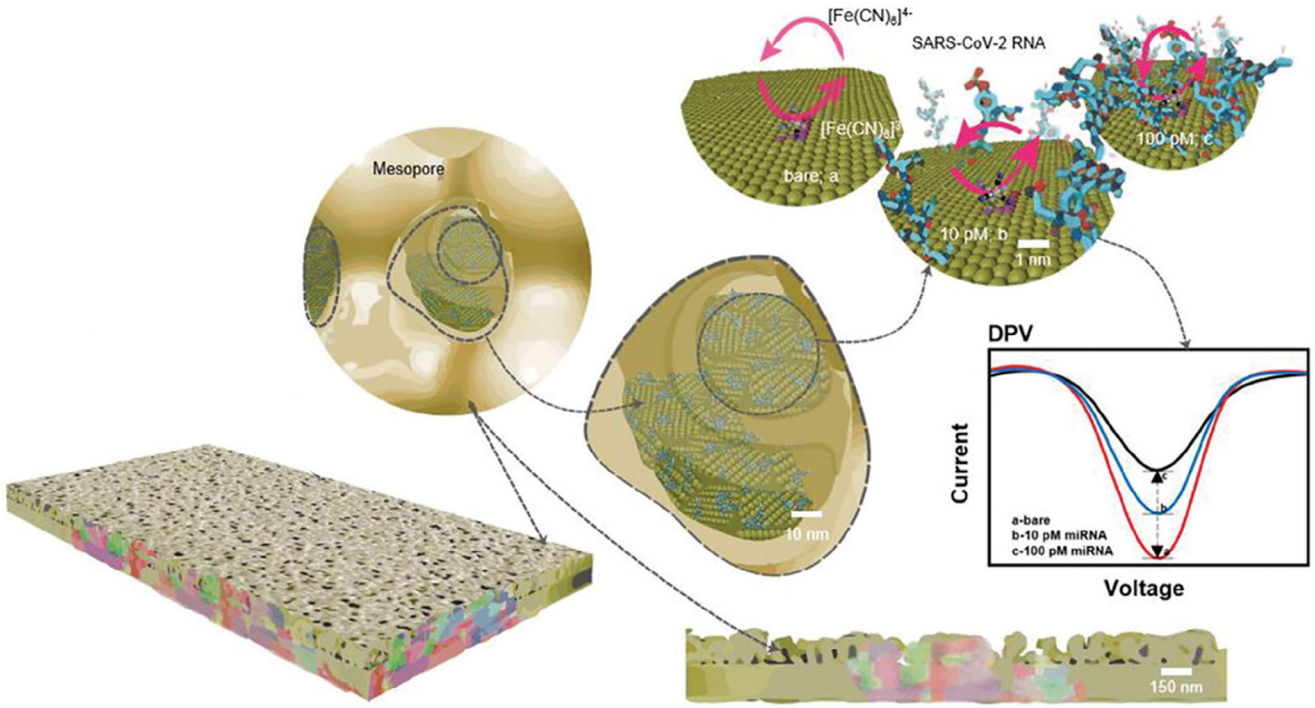

FIGURE 6 | Schematic illustration of the development of glass-grown mAu film for affinity-based electrochemical sensing of SARS-CoV-2-specific RNA without chemical and enzymatic amplification steps. A snapshot of assay construction to achieve attomolar affinity Au sensor for synthetic SARS-CoV-2; magnified images of the transducer surface during the electrochemical DPV interrogation at a level of micro- to nano-; representative readout for RNA adsorbed surface in the presence of redox molecules with bare, 10 pm, and 100 pm. Reproduced with permission [90]. Copyright 2024, Wiley.

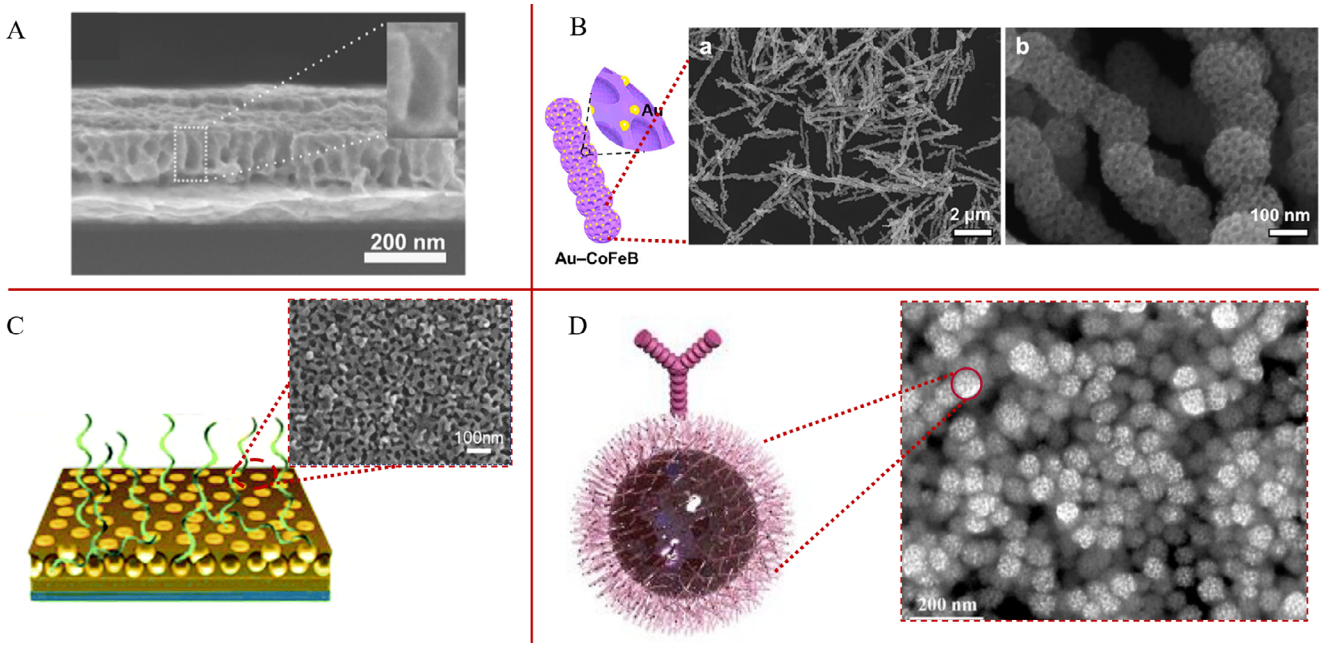

FIGURE 7 | (A) Cross-sectional SEM images of the mesoporous Au-Cu vertically oriented film. Reproduced with permission [98]. Copyright 2018, American Chemical Society. (B) Schematic illustration of the mesostructured Au–CoFeB and SEM images of mesoporous Au-CoFeB. Reproduced with permission [100]. Copyright 2023, American Chemical Society. (C) Schematic representation of the synthesised mesoporous Au–Ag alloy films with scanning electron microscopy (SEM) images of the mesoporous Au–Ag alloy. Reproduced with permission [95]. Copyright 2020, Royal Society of Chemistry. (D) Schematic illustration of the mesoporous trimetallic PdPtCu and SEM images of mesoporous PdPtCu. Reproduced with permission [101]. Copyright 2018, Elsevier.

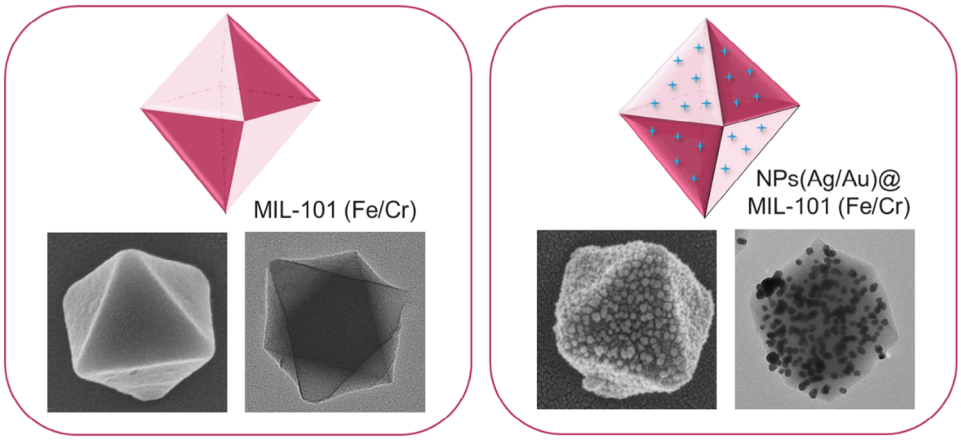

FIGURE 8 | Schematic illustration and SEM images of MIL-101(Fe)/MIL-101(Cr) and AgNPs@MIL-101(Fe)/AuNPs@MIL-101(Cr) morphology [118, 119]. Reproduced with permission [118]. Copyright 2022, Elsevier. Reproduced with permission [119]. Copyright 2022, Elsevier.

clusters coordinated with organic linkers. Owing to their tunable pore sizes, high surface areas, and accessible active sites, MOFs have found widespread applications in catalysis, energy storage, sensing, and drug delivery. However, most MOFs reported to date are microporous, with fewer examples of mesoporous (2–50 nm) or microporous structures [116]. The recent development of hierarchical porous MOFs incorporating micropores, mesopores, and/or macropores offers a promising strategy to broaden MOF functionality. These structures offer the potential to accommodate larger guest molecules, including metal nanoparticles and enzymes, which are often essential for biosensing applications [117–121].

Materials of Institute Lavoisier (MIL) based frameworks are well known for possessing both microporous and mesoporous structures [122, 123]. Among these MIL materials, MIL-101(Fe) and MIL-101(Cr) have a mesoporous architecture, enabling the diffusion of molecules through the pore channels, and exhibit good stability in water and across various pH conditions. These materials have been extensively implemented in electrochemical biosensors [118, 119, 124–126]. Further enhancement, such as decorating with gold/silver nanoparticles, as illustrated in Figure 8, could increase detection sensitivity, especially in surface-enhanced Raman spectroscopy [118, 119]. Owing to their tunable pore structure and electrocatalytic properties, mesoporous MOFs hold great promise for electrochemical biosensing and warrant further investigation.

Covalent organic frameworks (COFs) are a class of crystalline porous polymers that are composed of light elements (typically H, B, C, N, and O) linked by covalent bonds (—C—C—, —C═C—, —C═N—, -B-O-, etc.). Yaghi et al. introduced the synthesis of COFs (COF-1 and COF-5) via reversible chemical bonding, guided by the principle of topological design, in 2005 [127, 128]. With its special structure and excellent performance, COFs have shown good application potential in the fields of sensing and drug delivery, electrocatalysis, photocatalysis, energy storage and conversion, adsorption and separation, and gas storage [128–130]. We cannot find a record of mesoporous COFs being directly employed in electrochemical biosensors, likely due to their poor intrinsic conductivity and limited stability in electrochemical environments. However, tailoring their structures or hybridizing them with conductive nanomaterials could create new opportunities, leveraging the unique selectivity of mesoporous COFs for electrochemical biosensing.

Despite their structural versatility, the deployment of mesoporous materials in real-world biosensors is currently hindered by three fundamental bottlenecks: conductivity, selectivity, and stability. Mesoporous silica, while offering superior antifouling and gating capabilities, suffers from an inherent lack of conductivity. This insulating nature creates a high electron-transfer barrier that necessitates complex hybrid integration with conductive materials to function effectively as an electrochemical interface. Conversely, while mesoporous carbon and metals exhibit excellent conductivity, they often lack the intrinsic molecular sieving properties required to prevent biofouling in complex fluids like blood or sweat. Furthermore, the long-term stability of these high-surface-area scaffolds in physiological environments remains a critical concern, as pore collapse or surface degradation over time can lead to significant signal drift. Addressing these trade-offs, that is, balancing conductivity with selectivity and stability, remains the primary challenge for the next generation of material design.

In summary, each mesoporous structure has inherent advantages and disadvantages in application. The choice of a mesoporous material for biosensing is guided by the "Sensitivity-Selectivity Trade-off." While mesoporous carbon and metals offer superior sensitivity because of direct electron transfer capabilities, they inherently lack the size-exclusion properties necessary for analysing complex clinical fluids (e.g., blood, sweat, urine,a saliva) [69, 70, 79, 87]. Consequently, sensors based solely on conductive mesoporous scaffolds often suffer from biofouling and background noise in real-world settings. Conversely, while mesoporous silica and MOFs offer exceptional selectivity and anti-fouling properties through molecular sieving, their insulating nature necessitates the complex integration of heterogeneous materials with conductive substrates. Therefore, the future of clinical biosensing lies not in using these materials in isolation, but in hybrid architectures that couple the conductivity

of carbon/metals with the gating selectivity of silica/MOFs to resolve the interference challenges inherent to biological matrices. Table 1 lists these characteristics, along with the respective advantages and limitations of each mesoporous material.

4 | Fabrication of Mesoporous Material – Vertically-Oriented Silica Film

The common goal here is to construct open mesopores ranging from 2 to 50 nm in size. Typically, a "sacrificial material" is selected as a template to assemble with the material precursor to form a composite. Afterward, the template is removed, leaving behind mesopores in the spaces it once occupied. To date, a series of methods for the synthesis of mesoporous materials, particularly mesoporous silica nanoparticles, has been developed, including template-assisted methods, gel-processing synthesis, hydrothermal synthesis, and microwave synthesis [40, 44, 133].

4.1 | Template-Assisted Synthesis

Template-assisted synthesis of mesoporous materials employs templates to guide the specific pore morphology in the materials. To this end, the method uses surfactants, block copolymers (soft templates), or solid materials such as silica spheres (hard templates). Herein, template-assisted methods for the synthesis of mesoporous materials will be discussed. The soft template strategy typically comprises two major components: the soft template and the metal precursor, both dissolved in an aqueous medium. The soft template uses pore directors, such as block copolymers, surfactants, and supramolecular assemblies, as a core scaffold for the inorganic precursors (metal salts) reacting in the prepared solution. The hard-template approach for synthesizing mesoporous materials, also known as nanocasting, exo-templating, or the replicated template method, commonly employs silicas (e.g., KIT-6), polystyrene spheres, carbon nanotubes, and metal–organic frameworks as templates (Figure 9) [92, 134–136]. The skeleton precursors fill the gaps of the target material by heating and other treatments. Finally, after removal of the hard template as a sacrificial template by alkali etching, calcination, or other methods, a mesoporous metal oxide material/mesoporous carbon that replicates the hard template's pore structure is obtained (Figure 9).

4.2 | Gel Processing Synthesis

Gel processing synthesis is one of the feasible methods for synthesizing mesoporous materials, employing templates to guide the formation of desired pores and depositing a thin, uniform film of mesoporous metal, mesoporous alloys, or mesoporous silica on the working electrode surface. In general, the system undergoes a transformation from a liquid state (sol) to a solid phase (gel) during drying [40]. This technique involves evaporating a solution containing the precursor to form high-quality films on the surface. Mesoporous silica films (MSFs), one of the most widely studied types, are typically synthesised by preparing a precursor solution and then removing the template to reveal the porous structure. These films offer several benefits, including high chemical, thermal, and mechanical stability, as well as a large surface area, making them ideal for applications such as molecular sieving, catalyst supports, and enzyme immobilization. With advances in MSF technology, various electrochemical sensors have been developed, particularly those based on vertically ordered mesoporous silica films (VMSFs). These films exhibit unique structural and functional properties, making them suitable for biosensing and molecular separation. VMSF has the features of highly uniform pore sizes (2∼3 nm), ultrathin thickness (∼100 nm), and high porosity (∼10^{12} pores/cm^2). Their nanochannels are precisely aligned, either perpendicular or parallel to the electrode surface, and are rich in silanol groups (pK_a ∼2–3) [137]. In 2012, Zhao's research group introduced the Stöber method (Figure 10A) for fabricating VMSFs on negatively charged substrates, such as glass and ITO [138]. This method involves dissolving tetraethyl orthosilicate (TEOS) and CTAB in an ethanol-ammonia solution to create a precursor. CTAB micelles bind to the substrate via electrostatic forces, while TEOS slowly hydrolyses to form negatively charged silicate oligomers. These oligomers are attracted to the micelles. As ethanol diffuses into the micelles, their shape transitions from spherical to cylindrical. Ammonia facilitates hydrogen bonding between micelles and silicates, aiding this transformation. Continued diffusion and assembly lead to the deposition of silicates at the interface, forming the VMSF [138].

The drying process takes a substantial amount of time to achieve the desired film thickness. The electrochemically-assisted self-assembly (EASA) (Figure 10B) method offers a fast and effective way to produce VMSFs with highly ordered, hexagonally arranged nanochannels on conductive substrates [140]. In this process, a negative potential is applied to an electrode immersed in a pre-hydrolyzed precursor solution. Cationic surfactant micelles, typically formed from cetyltrimethylammonium bromide (CTAB), function as templates and rapidly self-assemble on the electrode surface. Simultaneously, the reduction of hydrogen ions and water generates hydroxide ions (OH^-), increasing the local pH and promoting silica condensation. Electrostatic interactions between negatively charged silica species and positively charged CTAB micelles lead to the rapid formation of a well-ordered mesoporous structure [139, 140].

In particular, VMSF grown on ITO substrates exhibits remarkable stability, attributable to the formation of covalent bonds between silica and surface hydroxyl groups. In contrast to ITO electrodes, commonly utilised carbonaceous or metallic electrodes show enhanced electrochemical activity but are constrained by insufficient adhesion to VMSF. The limited adhesion may significantly impair the sensitivity and selectivity of VMSF-based sensors. To address this predicament, molecular adhesives such as organosilanes, reduced graphene oxide (rGO) sheets and polydopamine have been documented to enhance the adhesion and long-term stability of VMSF on glassy carbon electrodes (GCE) or gold electrodes [141–143]. As of now, the rapid and straightforward fabrication of stable VMSF on electrodes characterized by high electrochemical and electrocatalytic activities without the employment of any adhesive agents remains a formidable challenge, even though this approach is both simple and effective in enhancing the sensitivity and selectivity of VMSF-based electrochemical sensors. Recent advancements in nanomaterials and surface modification techniques may provide innovative solutions for overcoming this challenge, potentially leading to the

TABLE 1 | Comparative analysis of mesoporous materials in electrochemical biosensing.

Mesoporous material class	Key properties	Role in Signal Transduction (Mechanism)	Key advantages	Key disadvantages	Refs.
Silica	**Insulating Support & Biocompatible Host** with vast silanol (-OH) groups for functionalization.	**Host Bioreceptors**: Provides a vast, stable 3D matrix for high-density enzyme/antibody immobilization. **Enhance Selectivity**: Acts as a molecular sieve, using pore size to physically block large interfering molecules (like proteins) from reaching the electrode.	**Excellent Functionalization**: Surface is easily modified via well-established silane chemistry for covalent bonding. **High Stability**: Chemically and thermally inert. **Biocompatible**: Ideal for enzyme encapsulation **Tunable Pores**: Pore size can be precisely controlled.	**Electrically Insulating**: This is the main drawback. The material creates a barrier to electron transfer that must be overcome, often by using it as a thin film or in a composite.	[7, 18, 131]
Carbon	**Conductive Scaffold & Surface Extender**	**Increase Electro-active Area**: Its high surface area boosts the current signal (capacitive and Faradaic).	**High Electrical Conductivity**: Its primary advantage for electrochemistry.	**Carbonization**: Requires high temperature to obtain carbonized material	[39, 69, 70]
Metals & Alloys	**Catalytic & Conductive Amplifier** Extremely high electrical conductivity and intrinsic catalytic activity	**Amplify Signal**: Catalyzes the electrochemical reaction of the analyte or a product. **Functionalization**: Functions as a 3D electrode, providing the best possible electrical contact for immobilized bio-receptors	**Highest Conductivity**: The best material for accelerating electron transfer. **Intrinsic Catalytic Activity**: Essential for many non-enzymatic sensors and for amplifying enzymatic signals	**Expensive**: Especially noble metals like Pt and Au.	[29, 79]
Metal Oxides	**Semiconducting & Catalytic Support** Semiconductors with unique electronic and catalytic properties.	**Act as Catalyst**: Many oxides, like (ZrO_2, CeO_2), have enzyme-like (nanozyme) activity, enabling non-enzymatic sensing.	**Versatile Electronics**: Can be semiconductors, catalysts, or magnetic (Fe_3O_4) for separation	**Stability Issues**: Can be pH-sensitive **Complex Electronics**: Semiconductor behavior can be complex	[39]
MOFs	**Ultra-High Surface Area & Tunable Host**	**Encapsulate**: Traps enzymes/bioreceptors within its crystalline pores, providing extreme protection and high loading capacity. **Pre-concentration**: Can be designed to selectively adsorb the target analyte, increasing its local concentration.	**Highest Surface Area**: Far exceeds all other classes. **Extreme Tunability**: Pore size, shape, and chemical functionality can be precisely designed by choosing different metals and linkers. **Redox-Active Centres**: The metal nodes can be redox-active (e.g., Fe) and participate in sensing.	**Lower Stability**: Often unstable in water, acidic, or basic solutions, which limits their use in biological buffers.	[118, 119, 132]

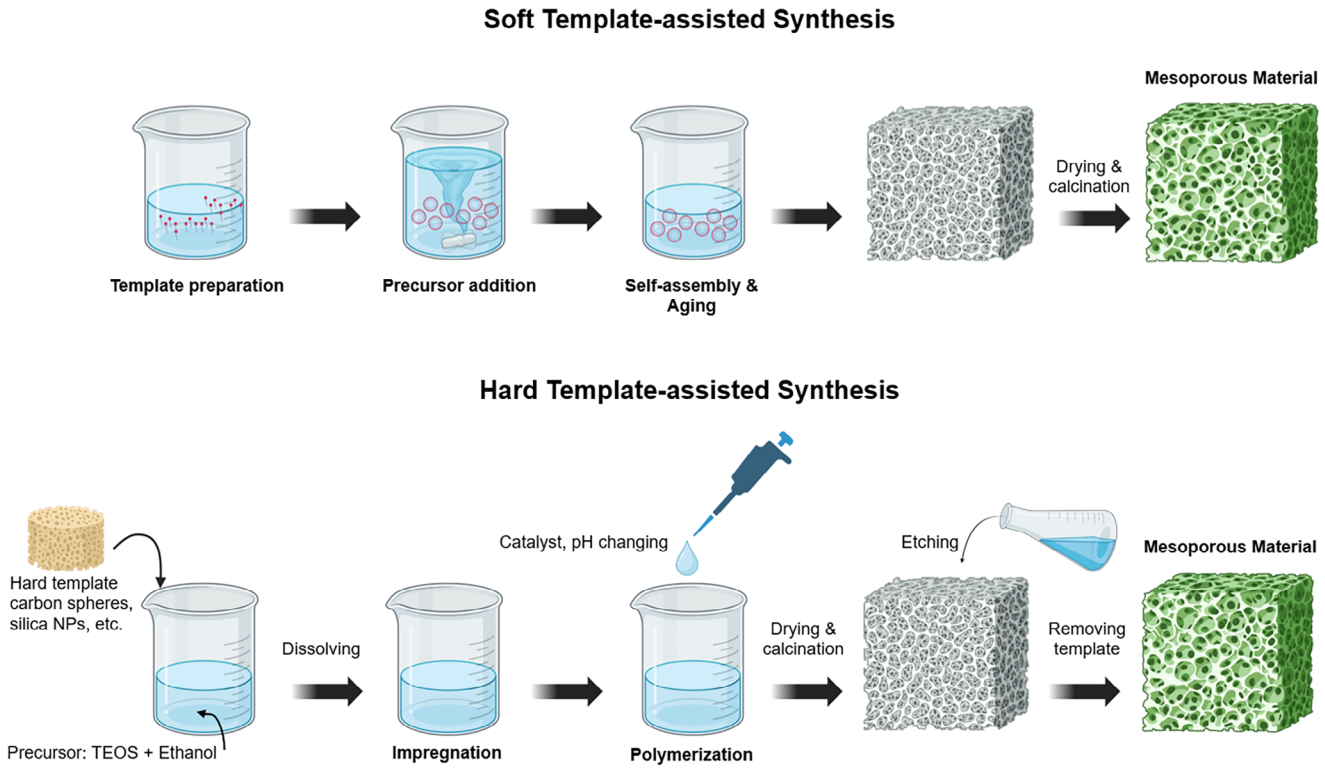

FIGURE 9 | Soft and hard template-assisted synthesis of mesoporous material.

development of more efficient and reliable VMSF-based sensors for various applications.

4.3 | Hydrothermal Synthesis

During hydrothermal synthesis, substances are chemically reacted with aqueous solutions at high temperature and high pressure in a sealed reaction chamber. The essence of this technique is the sol-gel process, but applying higher process intensity to produce mesoporous materials with improved regularity and hydrothermal stability [134, 144, 145]. Hydrothermal conditions, including temperature, pH, time, and reaction factors, can be adjusted to produce materials with specific pore sizes, pore volumes, and morphologies. In hydrothermal synthesis, organic template residues do not need to be removed after synthesis, unlike in templating methods [40].

4.4 | Microwave Synthesis

Microwave-assisted heating significantly accelerates the thermal processing and ensures uniform heating of samples. This method can penetrate deep into substances rather than relying on heat transfer. Therefore, the entire heating process can be completed in a considerably reduced timeframe compared to traditional processes. This characteristic results in a remarkably efficient heating process. Furthermore, the elevated efficiency of thermal

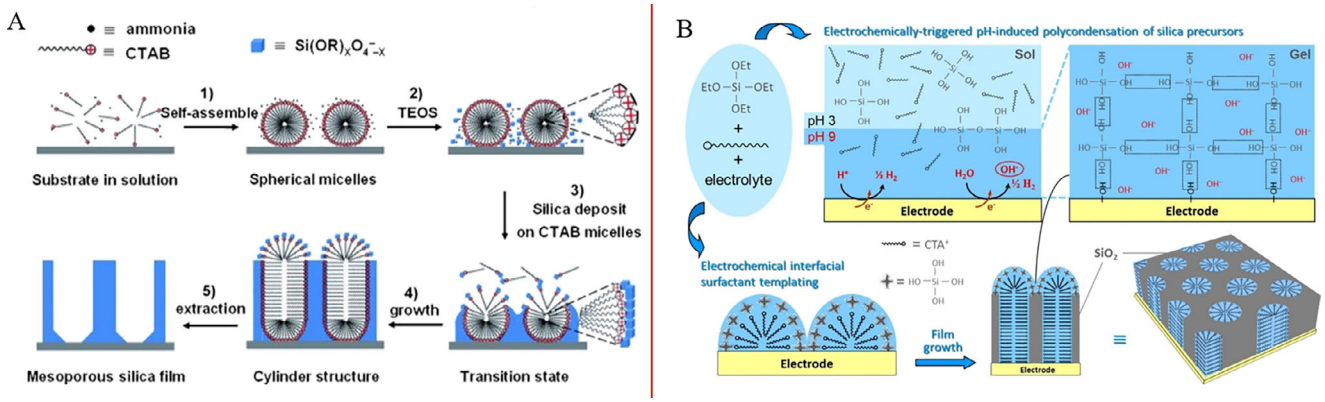

FIGURE 10 | (A) Schematic illustration of the formation process of VMSF by the Stöber-solution growth approach. Reproduced with permission [138]. Copyright 2012, John Wiley and Sons. (B) Schematic illustration of the EASA process for growth of VMSF. Reproduced with permission [139]. Copyright 2021, American Chemical Society.

energy utilization, along with the associated energy conservation, constitutes another salient feature of microwave synthesis in generating mesoporous materials. This efficiency is particularly advantageous in the synthesis of mesoporous materials, where rapid heating can improve structural integrity and uniformity throughout the material.

In contrast to sol–gel and electrochemically assisted routes widely used for vertically oriented mesoporous silica films, hydrothermal and microwave-assisted methods have predominantly been applied to mesoporous silica powders or nanoparticles. Recent reviews confirm that while microwave strategies enable rapid formation of mesoporous silica materials [146], hydrothermal treatments tune the pore structure of particles [147, 148]. Their application to film architectures (mainly vertically oriented mesoporous silica films) remains limited.

From a manufacturing perspective, the widespread adoption of mesoporous biosensors is limited by the incompatibility of traditional synthesis methods with modern device architectures. Conventional 'powder-based' strategies (e.g., hydrothermal synthesis) often rely on harsh chemical treatments or high-temperature calcination to remove templates. These aggressive processing conditions are fundamentally incompatible with the fragile, flexible substrates (such as plastics or textiles) required for wearable point-of-care devices [149]. Additionally, the physical integration of these powders onto electrodes (ohmic contact) typically requires insulating polymeric binders, which occlude pores and increase the interfacial charge transfer resistance (R_{ct}). Consequently, future fabrication efforts must pivot toward 'film-based' techniques like Electrochemically Assisted Self-Assembly (EASA). By enabling the direct, binder-free growth of mesoporous films under mild, room-temperature conditions, EASA effectively resolves the issues of substrate incompatibility and electrical contact that plague traditional methods.

5 | Mesoporous Silica Films as Functional Platforms in Electrochemical Biosensors

In the context of electrochemical biosensors, mesoporous silica is a highly desirable material compared to other mesoporous materials owing to its structural, chemical, and biological properties. The synthesis of mesoporous silica is characterized by a high degree of control and reproducibility, facilitating precise adjustment of pore dimensions, surface area, and film thickness through well-established soft or hard-templating methodologies. The surface of mesoporous silica is rich in silanol (-SiOH) groups, enabling straightforward and versatile functionalization with biomolecules such as enzymes, aptamers, and antibodies, thereby imparting selectivity in biosensing applications. In contrast to most mesoporous metals or metal-organic frameworks (MOFs), mesoporous silica offers intrinsic biocompatibility and non-toxicity [41, 58–60]. Moreover, vertically-ordered mesoporous silica films (VMSFs) exhibit remarkable antibiofouling capabilities by serving as size- and charge-selective barriers that obstruct larger or interfering entities, such as proteins, while permitting the diffusion of smaller target analytes, as discussed in the antibiofouling membrane section [150–153]. Although silica is recognized for its electrical insulating properties, this aspect can be advantageous when integrated with conductive substrates (e.g., gold, carbon, indium tin oxide), as it mitigates unwanted background signals and facilitates controlled electrochemical responses. The convenience of synthesis, potential for functionalization, structural tunability, anti-fouling attributes, and compatibility with a variety of electrode systems position mesoporous silica as a robust candidate material for electrochemical biosensors.

5.1 | Anti-Biofouling Membrane

An anti-biofouling membrane composed of mesoporous silica thin films serves as an intelligent, adjustable, non-conductive barrier that inhibits nonspecific adsorption of proteins, cells, and other biomolecules while facilitating the selective diffusion of target analytes. This characteristic is of paramount importance for electrochemical biosensors operating in complex biological fluids such as sweat, urine, saliva, whole blood, and plasma. In recent years, various antifouling molecules and materials, including self-assembled monolayers, peptides, proteins, zwitterions, and poly(ethylene glycol)-based polymers, have been utilised to construct low-fouling electrodes for in vitro electroanalysis in complex biological samples [154, 155]. While these approaches improve the antifouling performance of electrodes, they can also impede mass and charge transport, thereby limiting sensing efficiency. To address these limitations, mesoporous silica membranes have emerged as a promising alternative, offering both electrostatic enrichment and intrinsic antifouling properties [150–153]. The anti-biofouling property is attributed to the highly ordered mesoporous architecture of mesoporous silica films, with pore sizes typically ranging from 2 to 10 nm and pore densities up to $10^{12}/cm^2$. This structure serves as a molecular sieve, permitting the passage of small analytes (e.g., glucose, dopamine, uric acid, hydrogen peroxide) while blocking larger fouling species, such as proteins (e.g., bovine serum albumin, ~7 nm). Consequently, the prevention of pore clogging and maintenance of long-term sensor performance are principal features of the anti-biofouling mechanism as listed in Table 2.

The antifouling capability of VMSFs has been widely demonstrated in recent studies. Zhou et al. reported high-performance antifouling Carbon Fiber Microelectrodes (CFMEs) modified with antifouling Surface Nanomaterials (SNM) based on silica, characterized by their ultrasmall dimensions, uniformity, closely packed structure, and vertical alignment of channels. In both in vitro and in vivo experimental settings, SNM demonstrated a remarkable capacity to inhibit severe biofouling of the underlying electrode surface while maintaining high oxygen (O2) permeability. A simplified brain oxygen model was utilised to assess the antifouling efficacy of SNM/CFMEs. While non-invasive methodologies such as magnetic resonance imaging can detect or even map oxygen concentrations within the brain, the present methodology has the potential to be extended to detect a diverse array of electro-active species, including dopamine, uric acid, ascorbic acid, and reactive oxygen species [157].

Another showcase of small-molecule detection is the study by Xuan et al., which presents a strategy for fabricating VMSF on a glassy carbon electrode (GCE) without chemical adhesives, thereby enhancing adhesion and stability (Figure 11A) [156]. The

TABLE 2 | Examples of label-free detection via mesoporous silica structures for electroactive biomolecules.

Analyte	Electrode configuration	Concentration range	LoD	Sensitivity	Refs.
H_2O_2	AgNPs@VMSF/CFME	0.1–200 μM	25.3 nM	—	[25]
H_2O_2	Pt NPs@VMSF/ITO	10–500 μM	—	43.32 μM/mM	[155]
Dopamine	VMSF/p-GCE	10 nM–1.0 μM 1.0–30 μM	0.88 nM	6.80 μA/μM 4.06 μA/μM	[156]
Dopamine	Ru@VMSF/ITO	5 nM–20 μM	3.5 nM	—	[15]
Uric acid	NH_2-VMSF/3DG@CNT/GCE	0.1–50 μM	6.8 nM	1.66 μA/μM	[16]
Uric acid	NH_2-VMSF/ErGO/SPCE	0.5–100 μM	6.8 nM	0.144 μA/μM	[17]
Noradrenaline	Au NPs@NH_2-VMSF/p-GCE	50 nM–2 μM 2–50 μM	10 nM	1.44 μA/μM 0.76 μA/μM	[142]
Glucose	GDH/O-VMSF/ITO	10 nM–1 mM	1.5 nM	—	[21]

CFME: carbon fiber microelectrode, **GDH**: glucose dehydrogenase, **SPCE**: screen-printed carbon electrode, **ITO**: indium tin oxide, **FTO**: fluorine-doped tin oxide, **p-GCE**: pretreated-glassy carbon electrode, **ErGO**: electrochemically reduced graphene oxide, **3DG@CNT**: 3D graphene-carbon nanotubes.

team introduced hydroxyl groups onto the surface of GCE (p-GCE) before depositing VMSF on electrode. This approach could overcome the existence of chemical adhesives between GCE and VMSF. VMSF/p-GCE shows high sensitivity for dopamine detection in serum samples under optimal conditions including pH 6.0 and 20 s preconcentration time. The sensor also exhibited excellent anti-fouling and anti-interference properties offered by VMSF [156]. Similarly, Ma et al. developed a reliable and miniaturized electrochemical sensor for the sensitive detection of uric acid (UA) in human whole blood, utilising a screen-printed

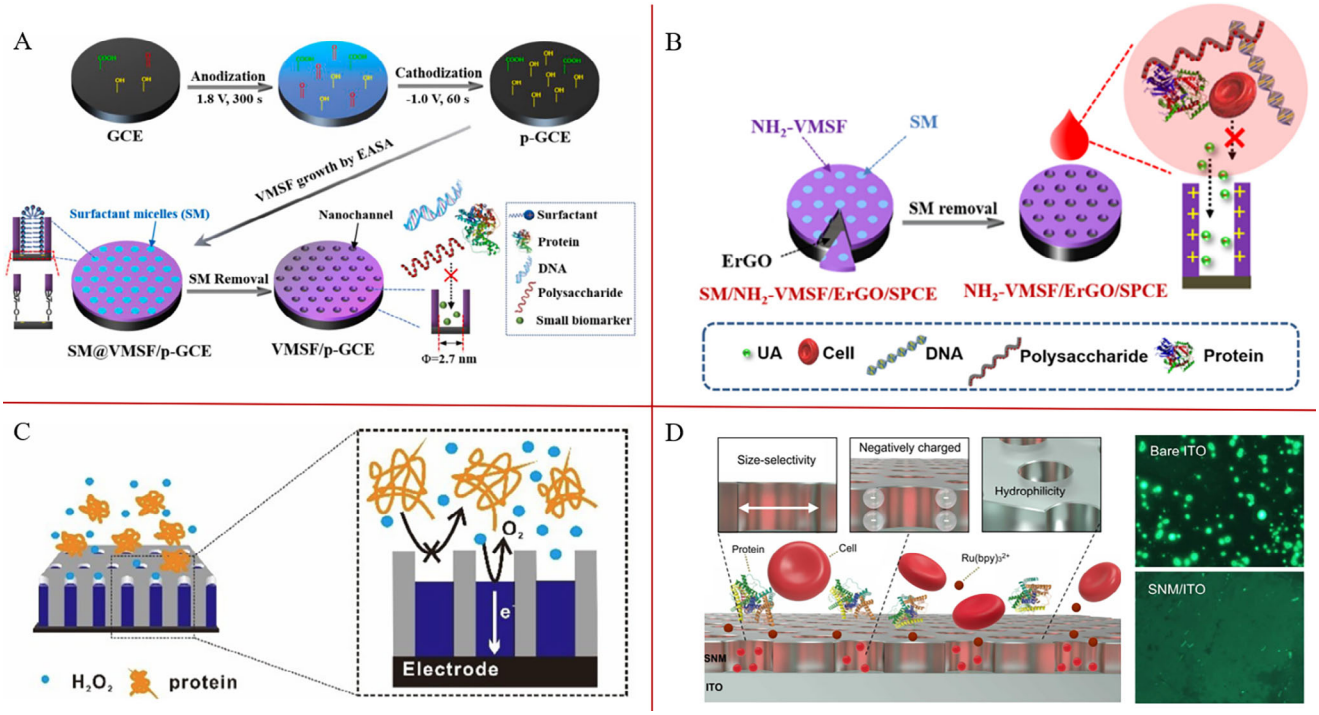

FIGURE 11 | (A) Schematic illustration for the preparation of p-GCE and subsequent growth of VMSF on the electrode by EASA. Reproduced with permission [156]. Copyright 2021, Elsevier. (B) Schematic illustration of the stable coupling of NH_2-VMSF with SPCE using ErGO as an adhesive layer and direct uric acid detection of human whole blood. Reproduced with permission [17]. Copyright 2021, MDPI AG. (C) Illustration of a low-fouling Pt@SNM coated electrode for H_2O_2 detection, preventing protein clogging of the electrode. Reproduced with permission [155]. Copyright 2020, John Wiley and Sons. (D) Illustration of size-selective, negatively charged, and hydrophilic SNM/ITO for Dopamine detection in complex bio-samples and fluorescent images of ITO and SNM/ITO surface before and after FITC-BSA treatment. Reproduced with permission [15]. Copyright 2022, Elsevier.

carbon electrode (SPCE) modified with a VMSF (Figure 11B) [17]. The integration of VMSF with SPCE not only enhanced sensitivity and selectivity through molecular sieving and antifouling effects but also enabled practical use in complex biological samples owing to the portability and cost-effectiveness of SPCE platforms [17].

Taking advantage of the anti-biofouling characteristics of nanoporous silica layer, Zhu et al. developed a fully integrated device with indium tin oxide glass electrode for ECL detection of dopamine in complex biological samples. Their approach afforded detection of dopamine with a linear range of 5 nM to 20 μM and a detection limit of 3.5 nM in urine and rat brain homogenates [15]. The anti-biofouling properties were attributed to negatively charged silica layer and electrostatic repulsion of negatively charged proteins, as depicted in Figure 11D [15]. Continuing this approach, Cui et al. presented a rapid and convenient electrochemical method for the highly sensitive detection of uric acid (UA) using a novel integration of vertically-ordered mesoporous silica film bearing amino groups (NH_2-VMSF) and a three-dimensional graphene-carbon nanotubes (3DG@CNT) composite film [16]. NH_2-VMSF, which contained amino groups, was grown on the 3DG@CNT/GCE surface through a one-step condensation process, providing a positively charged microenvironment that facilitates the electrostatic enrichment of anionic species like uric acid. The combination of the high electrocatalytic activity of 3DG@CNT and the electrostatic preconcentration ability of NH_2-VMSF resulted in a sensor capable of highly sensitive electrochemical detection of UA in blood sample and urine [16].

The oxidation ability of noble metals such as platinum, nickel, and gold enables their infiltration into the nanochannels of VMSFs. This process results in homogeneous dispersion, which enhances the catalytic and electrochemical performance of the modified electrodes. Moreover, the molecular sieving effect and high permeability of VMSFs, enabled by their uniform channels, vertical orientation, and tunable porosity, afford electrodes with excellent antifouling properties [15, 25, 142, 155].

Fabrication of platinized silica nanoporous membrane (Pt@VMSF) on carbon fiber microelectrode (CFME) was reported by Li et al. and shown in Figure 11C [155]. The incorporation of a nanoporous structure effectively confines the electrodeposition of platinum nanostructures while simultaneously preventing the adsorption of fouling species on the underlying electrode. This effectively enhances the sensor's antifouling properties. The CFME modified with Pt NPs@VMSF was utilised to monitor H_2O_2 concentration. Experimental evidence demonstrated that this electrode could function stably in the cortical layer of rat brains for up to 90 min [155]. Similarly, Huang et al. developed an electrochemical sensor for the sensitive detection of noradrenaline in human whole blood, a neurotransmitter and hormone crucial in pain-related processes [142]. The sensor utilised a pre-activated glassy carbon electrode modified with vertically ordered silica nanochannels and in situ-deposited gold nanoparticles (AuNPs). The sensor demonstrated a wide detection range for noradrenaline, a low limit of detection, high selectivity, ease of regeneration, and the capability for direct analysis in human whole blood samples [142].

5.2 | "Targeting" by Functionalization for Electrochemical Immunosensors and Aptasensors

Antibodies—immune system proteins generated in response to specific antigens- are considered the "gold standard" of molecular recognition elements and remain central to molecular biology. Their high binding specificity has enabled widespread applications in natural and medical sciences [158]. Nucleic acid aptamers are oligonucleotide sequences comprising approximately 25–80 nucleotides that bind target molecules with high specificity, an ability comparable to that of monoclonal antibodies [159, 160]. Aptamers are gaining considerable attention in clinical applications due to their distinct advantages, including long-term stability, minimal batch-to-batch variation, low immunogenicity, ease of chemical modification, extended serum half-life, and enabling targeted delivery. Aptamers offer several benefits over protein-based ligands for use as research tools and therapeutics. Comparable to monoclonal antibodies in terms of binding affinity, aptamers can instead be stored at room temperature and reversibly denatured in solution. Moreover, as nucleic acids, they can be synthesised in large quantities by solid-phase synthesis, readily purified, and easily subjected to site-specific chemical conjugation [161–164].

Mesoporous silica, while inherently unable to selectively recognize specific biological targets, offers highly advantageous surface chemistry for biosensing applications. Its densely packed and uniformly distributed silanol groups (-SiOH) on both the surface and within the pore channels provide a reactive platform for further chemical modification. Through silanization techniques using organosilanes such as (3-aminopropyl)triethoxysilane (APTES) or (3-aminopropyl)trimethoxysilane (APTMS) [165–167], covalent bonds can be formed between the silica framework and functional biomolecules such as aptamers and antibodies, using linking molecules such as EDC/NHS or glutaraldehyde [168]. This capability transforms mesoporous silica into a versatile scaffold for the construction of highly selective electrochemical biosensors, including aptasensors and immunosensors.

Importantly, aptamers and antibodies provide *targeting capability* by selectively capturing analytes of interest, thereby offering mesoporous silica–based sensors with molecular specificity. The binding events can act as a gating effect, modulating access to the mesoporous channels in response to target molecules. This "bio-gating effect" represents a powerful mechanism to achieve selective detection and will be discussed in detail in the following section.

5.3 | Detection Strategy via Gating Effect

The integration of antibodies and aptamers with mesoporous silica offers a powerful strategy for enhancing biosensor performance. While antibodies and aptamers provide high binding affinity and molecular selectivity toward target analytes, the abundant surface silanol groups of mesoporous silica create a versatile platform for chemical functionalization. This combination not only maximizes biorecognition capability but also

TABLE 3 | Application of mesoporous silica films integrated with aptamers and antibodies.

Analyte	Electrode configuration	Recognition molecule	Concentration range	LoD	Refs.
PSA	Apt/VMSF/Au	Aptamer	1 – 300 ng/mL	280 pg/mL	[166]
PSA	VMSF/ITO	Antibody	1 pg/mL—100 ng/mL	0.1 pg/mL	[169]
SARS-CoV-2-RBD	Apt/MB@VMSF/LEGE	Aptamer	0.5 – 250 ng/mL	0.36 ng/mL	[170]
SARS-CoV-2 IgG	Ru@bp-SNA/ITO	Antibody	0.5 pg/mL—1 μg/mL	2.9 pg/mL	[171]
cTnI	Apt/APTMS/VMSF/ITO	Aptamer	0.05 pg/mL—1 ng/mL	0.02 pg/mL	[165]
CEA **CA15-3**	Ag/Ab/Ru@bp-SNA/ITO	Antibody	0.0001 – 50 ng/mL 0.005 – 500 U/mL	0.06 pg/mL 0.0023 U/mL	[172]
CEA	Apt/GA/MB@bp-SNA/ITO	Aptamer	1 pg/mL—1 μg/mL	0.22 pg/mL	[173]
CA 15-3	Anti-CA 15-3/O-VMSF/ITO	Antibody	0.1 mU/mL – 100 mU/mL (ECL) 10 mU/mL – 200 U/mL (EC)	9 μM/mL (ECL) 5.4 μM/mL (EC)	[174]
Cortisol	cDNA/Aptamer/VMSF/ITO	Aptamer/cDNA	10 – 5000 nM	8 nM	[22]

PSA: prostate-specific antigen, **SARS-CoV-2-RBD**: severe acute respiratory syndrome coronavirus-2-receptor binding domain, **SARS-CoV-2 IgG**: severe acute respiratory syndrome coronavirus-2-immunoglobulin G antibody, **cTnI**: Cardiac Troponin I, **CEA**: carcinoembryonic antigen, **CA 15-3**: cancer antigen 15-3, **Apt**: aptamer, **Ab**: antibody, **bp-SNA**: bipolar silica nanochannel arrays, **LEGE**: laser engraved graphene electrode, **GA**: glutaraldehyde, **cDNA**: complementary DNA, **EC**: electrochemical, **ECL**: electrochemiluminescence, **MB**: methylene blue.

leverages the large surface area and tunable porosity of the silica film, enabling dense probe immobilization and amplified signal transduction, as summarized in Table 3.

VMSFs act as nanogates, with their uniform, highly ordered channels selectively regulating the diffusion of electroactive species toward the electrode surface. The functionalization of nanochannels with aptamers or antibodies further strengthens this concept. These bioreceptors act as molecular 'gates' that specifically open or close access to the electrode surface in the presence of target analytes [165, 174]. Mi et al. reported a dual-modular aptasensor for the accurate determination of cardiac troponin I (cTnI), which serves as a critical biomarker indicative of acute myocardial infarction. This system exhibited concurrent outputs of electrochemiluminescence (ECL) and electrochemical impedance spectroscopy (EIS) that are predicated on target-gated transport mechanisms of signalling probes (luminol/H_2O_2 or $Fe(CN)_6^{3-/4-}$) [165]. Huang et al. introduced a dual-mode sensing platform that combines electrochemiluminescence and electrochemistry for the sensitive and selective determination of cancer antigen 15-3 (CA 15-3), a specific biomarker for breast cancer [174].

The prostate-specific antigen (PSA) test is widely used for prostate cancer screening, serving as an initial indicator of patients who may require further diagnostic evaluation [166, 169, 175]. Argoubi et al. reported a novel label-free electrochemical aptasensing platform for the detection of PSA, using mesoporous silica thin-film-coated gold electrodes [166]. In a similar approach to the gating effect, Ma et al. grew VMSF with high surface area and negative charge on ITO electrodes, which significantly enhanced ECL emission by strongly attracting positively charged $(Ru(bpy)_3^{2+})$ ions and thereby improving the sensor's sensitivity [169]. The PSA antibody was covalently modified with epoxy groups on the surface of VMSF to construct a gated ECL detection platform. It provided a new way to detect biomarkers in human serum samples, rapidly and sensitively [169].

Mesoporous silica films possess excellent encapsulation ability, allowing biomolecules, nanoparticles, and catalysts to be confined within their uniform nanochannels or cavities, as shown in section 4.1 [170–173]. Building on this concept, with gating to encapsulate the probe within the nanochannels, Tabrizi and Acedo presented a novel aptasensor specifically designed for the detection of the receptor-binding domain of SARS-CoV-2 (SARS-CoV-2-RBD) using a unique combination of a mesoporous silica film and aptamer technology [170]. This aptasensor optimized methylene blue (MB) encapsulated within the mesoporous silica film, which acts as a probe molecule, while the aptamer served as a bio-gatekeeper, enhancing the specificity and sensitivity of the detection method [170].

The bipolar silica nanochannel array, formed by sandwiched layers of VMSF with opposite surface charges, allows the encapsulation of probe molecules via dual electrostatic forces. This approach can be used to encapsulate probe molecules such as methylene blue and (tris(2,2′-bipyridyl)ruthenium (II)) $(Ru(bpy)_3^{2+})$ within the nanochannels of VMSF with opposite surface charges. A showcase is presented by Gong et al., who develop a solid-state electrochemiluminescence (ECL) platform specifically designed for the detection of SARS-CoV-2 antibodies [171]. The platform demonstrates the ability to detect SARS-CoV-2 IgG with a wide linear range and a low limit of detection, along with a short incubation time, which signifies its

efficiency and practicality. Building on this concept, Gong et al. introduced a dual-mode electrochemiluminescence (ECL) and electrochemical (EC) sensing platform utilising a bipolar silica nanochannel array (bp-SNA) confined with a bifunctional probe, $Ru(bpy)_3^{2+}$ [172]. The platform demonstrates high sensitivity and selectivity for tumor-related biomarkers, including carcinoembryonic antigen (CEA) and cancer antigen 15-3 (CA15-3) [172]. Similarly, Zhou et al. introduced a novel probe-integrated aptamer sensor for the reagent-less electrochemical detection of the tumor biomarker carcinoembryonic antigen (CEA) [173]. This sensor utilised the same bipolar silica nanochannel film (bp-SNF), which enabled the stable confinement of the electrochemical probe methylene blue (MB) via dual electrostatic interactions, thereby enhancing detection sensitivity. The sensor provided a micro-structured electrode surface that significantly increases the density of fixed electrochemical probes, thereby enhancing performance, selectivity, and stability in serum detection [173].

5.4 | Integration in a Point-of-Care Device

With the growing demand for rapid, real-time, and non-invasive health monitoring, the integration of mesoporous silica thin films into point-of-care (POC) and wearable devices has become increasingly urgent. The unique structural features of vertically ordered mesoporous silica films (VMSF)—including uniform nanochannels, high surface area, tunable pore size, and the rich presence of reactive silanol groups—make them highly attractive for functionalizing with biomolecular recognition elements such as aptamers and antibodies. These films offer not only enhanced molecular selectivity and signal amplification but also inherent antibiofouling properties, which are essential for reliable performance in complex biological matrices such as sweat, saliva, or interstitial fluid. Moreover, their excellent chemical and thermal stability support long-term use in flexible, miniaturized platforms. Recent advancements have demonstrated the feasibility of integrating mesoporous silica coatings onto microelectrodes and wearable patches, achieving sensitive and selective detection of biomarkers such as glucose and cortisol in human sweat [15, 22]. These efforts underscore the material's potential to serve as a foundational component for next-generation personalized healthcare tools, enabling early disease detection, continuous health monitoring, and accessible diagnostics beyond conventional clinical settings.

6 | Perspectives and Conclusion

Mesoporous materials have emerged as exceptionally versatile and powerful platforms for enhancing the performance of electrochemical biosensors. This is mainly due to their remarkably high surface area, tunable pore structures, and extensive chemical functionalization. The integration of mesoporous scaffolds—such as silica, carbon, and metal oxides -has led to significant advancements in sensor sensitivity, selectivity, and stability. These improvements stem from enhanced biomolecule immobilization, more controlled analyte transport, and superior antifouling properties, which collectively contribute to more reliable and accurate biosensing.

Among the several types of mesoporous materials, mesoporous silica, particularly in the form of VMSFs, distinguishes itself due to its excellent processability, reproducibility, and compatibility with a diverse array of electrochemical transducers. The presence of surface silanol groups on these silica structures facilitates strong covalent bonding to functional elements, such as aptamers and antibodies. This characteristic is crucial for the development of both aptasensors and immunosensors, which can target a broad spectrum of biological analytes, ranging from small molecules to large biomolecules.

Despite their remarkable surface area, tunable porosity, and chemical versatility, mesoporous materials face several intrinsic limitations that hamper their full potential in electrochemical biosensing applications. The most critical challenge is poor electrical conductivity, particularly in insulating frameworks such as mesoporous silica and MOFs [7, 18, 118, 119, 131, 132]. These materials can form electron-transfer barriers when used as thick coatings, thereby attenuating the electrochemical signal. To address this issue, composite formation with conductive additives such as gold nanoparticles [119, 143], integration with conductive materials such as mesoporous carbon or conversion of insulating structures (e.g. MOFs) into conductive carbons through pyrolysis, could enhance conductivity. In some cases, thin-film deposition is also used to minimize the tunneling distance for electron transfer.

The pore size of mesoporous materials plays a crucial role in determining their performance, depending on the intended analytical application. Typically, the pore diameter should exceed the size of the immobilized biomolecules—such as enzymes, aptamers, antibodies, or analytes—to ensure efficient loading and accessibility. However, excessively large pores can lead to leaching, non-specific absorption, and reduced catalytic activity, highlighting the importance of size compatibility. Conversely, mesoporous layers with smaller pore sizes can act as protective barriers, shielding the transducer from interferences while enhancing the stability and activity of the assembled biosensor. Therefore, the rational design of mesoporous matrices with optimal pore dimensions is essential to balance biomolecule loading, retention, and functional stability, thereby achieving superior sensing performance.

Despite the substantial progress in this field, several challenges persist. Achieving high specificity and reproducibility in the complex, often heterogeneous environments of biological samples requires further refinement of surface chemistry, pore architecture, and anti-fouling strategies. Moreover, the transition from laboratory-scale devices to practical, real-world applications is often hindered by concerns about long-term stability, reusability, cost-effectiveness, and the feasibility of large-scale manufacturing.

Looking ahead, the future development of mesoporous material-based electrochemical biosensors is anticipated to align with several key technological and clinical trends. First, there is a growing emphasis on integration into point-of-care and wearable systems. The miniaturization and mechanical flexibility of mesoporous thin films render them particularly suitable for on-body applications. Future research should prioritize the development of flexible substrates, microfluidic interfaces, and

wireless readout systems that enable real-time, continuous health monitoring.

Additionally, the potential for multiplexed and multimodal sensing is significant. By incorporating multiple recognition elements into a single mesoporous scaffold, it may be possible to detect multiple biomarkers simultaneously. This capability could greatly enhance diagnostic accuracy while reducing testing time.

Sustainable and scalable synthesis approaches are also crucial for the future commercialization of these biosensors. The exploration of environmentally friendly, cost-effective fabrication methods, such as template-free processes, room-temperature synthesis, and additive manufacturing-compatible techniques, will be essential to addressing current limitations. Furthermore, the design of innovative and responsive materials that exhibit property changes in response to stimuli such as pH, temperature, or specific biomolecular interactions could open new avenues for dynamic sensing applications and targeted drug delivery systems.

Finally, the integration of machine learning and data analytics into biosensing technologies holds promise for enhancing signal accuracy and supporting predictive diagnostics in personalized medicine. By coupling advanced biosensors with AI-driven interpretation tools, we can expect significant improvements in the overall efficacy and reliability of diagnostic systems.

In conclusion, mesoporous materials, particularly those utilising scaffold-based architectures, are poised to play a pivotal role in advancing electrochemical biosensors toward real-world deployment. By bridging the gap between innovative nanomaterials and comprehensive system-level integration, the next generation of biosensors is set to revolutionize diagnostics, health monitoring, and disease management across both clinical and non-clinical settings.

Author Contributions

Vinh Khanh Ho: Writing – review & editing, Writing – original draft, Validation, Investigation, Conceptualisation. **Tuan-Khoa Nguyen**: Supervision, Review & editing. **Sina Jamali**: Validation, Supervision, Conceptualisation, Review & editing. **Nam-Trung Nguyen**: Validation, Supervision, Conceptualisation, Review & editing, Project administration. All authors participated in the critical review process of the manuscript. All authors read and approved the final manuscript.

Acknowledgements

The authors thank the Queensland Quantum and Advanced Technologies Research Institute, the School of Engineering and Built Environment, and the School of Environment and Science at Griffith University for providing the necessary infrastructure and facilities. V.K. Ho and N.-T. Nguyen acknowledge funding from the Australian Research Council through the Australian Laureate Fellowship (FL230100023). The authors also acknowledge M. A. Huynh for drawing Figure 1. S. Jamali acknowledges funding from the Australian Research Council (ARC), Discovery Early Career Researcher Award (DECRA) DE210101137. T. -K. Nguyen acknowledges the support from the Australian Research Council (ARC) DECRA Fellowship (DE240100408).

Open access publishing facilitated by Griffith University, as part of the Wiley - Griffith University agreement via the Council of Australian University Librarians.

Funding

The Australian Research Council supports the project through the Australian Laureate Fellowship (FL230100023) to N.T.N.

Conflicts of Interest

The authors declare no conflicts of interest.

Data Availability Statement

The authors have nothing to report.

References

1. J. Kim, A. S. Campbell, B. E.-F. de Ávila, and J. Wang, "Wearable Biosensors for Healthcare Monitoring," *Nature Biotechnology* 37 (2019): 389–406, https://doi.org/10.1038/s41587-019-0045-y.

2. J. Wu, H. Liu, W. Chen, B. Ma, and H. Ju, "Device Integration of Electrochemical Biosensors," *Nature Reviews Bioengineering* 1 (2023): 346–360, https://doi.org/10.1038/s44222-023-00032-w.

3. H. Costanzo, J. Gooch, and N. Frascione, "Nanomaterials for Optical Biosensors in Forensic Analysis," *Talanta* 253 (2023): 123945, https://doi.org/10.1016/j.talanta.2022.123945.

4. T. T. Nguyen, C. M. Nguyen, M. A. Huynh, H. H. Vu, T. K. Nguyen, and N. T. Nguyen, "Field Effect Transistor Based Wearable Biosensors for Healthcare Monitoring," *Journal of Nanobiotechnology* 21 (2023): 411, https://doi.org/10.1186/s12951-023-02153-1.

5. X. Jin, A. Cai, T. Xu, and X. Zhang, "Artificial Intelligence Biosensors for Continuous Glucose Monitoring," *Interdisciplinary Materials* 2 (2023): 290–307, https://doi.org/10.1002/idm2.12069.

6. H. Meskher, S. B. Belhaouari, and F. Sharifianjazi, "Mini Review About Metal Organic Framework (MOF)-based Wearable Sensors: Challenges and Prospects," *Heliyon* 9, no. 11 (2023): 21621, https://doi.org/10.1016/j.heliyon.2023.e21621.

7. C. Erkmen, V. Sanko, B. O. Ozturk, J. Quinchía, J. Orozco, and F. Kuralay, "Mesoporous Silica-based Electrochemical Biosensors in the Determination of Cancer Biomarkers: Current Progress on Analytical Performance and Future Trends," *TrAC Trends in Analytical Chemistry* 179 (2024): 117876, https://doi.org/10.1016/j.trac.2024.117876.

8. R. Sarkhosh-Inanlou, V. Shafiei-Irannejad, S. Azizi, et al., "Applications of Scaffold-based Advanced Materials in Biomedical Sensing," *TrAC Trends in Analytical Chemistry* 143 (2021): 116342, https://doi.org/10.1016/j.trac.2021.116342.

9. M. P. Nikolova and M. S. Chavali, "Recent Advances in Biomaterials for 3D Scaffolds: A Review," *Bioactive Materials* 4 (2019): 271–292, https://doi.org/10.1016/j.bioactmat.2019.10.005.

10. C. Verma, E. Berdimurodov, D. K. Verma, K. Berdimuradov, A. Alfantazi, and C. M. Hussain, "3D Nanomaterials: The Future of Industrial, Biological, and Environmental Applications," *Inorganic Chemistry Communications* 156 (2023): 111163, https://doi.org/10.1016/j.inoche.2023.111163.

11. H. Cheng, W. Li, S. Duan, et al., "Mesoporous Silica Containers and Programmed Catalytic Hairpin Assembly/Hybridization Chain Reaction Based Electrochemical Sensing Platform for MicroRNA Ultrasensitive Detection With Low Background," *Analytical Chemistry* 91 (2019): 10672–10678, https://doi.org/10.1021/acs.analchem.9b01947.

12. H.-J. Pan, Y.-C. Gong, W.-Q. Cao, et al., "Fascinating Immobilization-Free Electrochemical Immunosensing Strategy Based on the Cooperation of Buoyancy and Magnetism," *Analytical Chemistry* 95, no. 18 (2023): 7336–7343, https://doi.org/10.1021/acs.analchem.3c00485.

13. A. Zhu, T. Jiao, S. Ali, Y. Xu, Q. Ouyang, and Q. Chen, "SERS Sensors Based on Aptamer-Gated Mesoporous Silica Nanoparticles for Quantitative Detection of Staphylococcus aureus With Signal Molecular Release," *Analytical Chemistry* 93 (2021): 9788–9796, https://doi.org/10.1021/acs.analchem.1c01280.

14. J. Guo, S. Chen, S. Tian, K. Liu, X. Ma, and J. Guo, "A Sensitive and Quantitative Prognosis of C-reactive Protein at Picogram Level Using Mesoporous Silica Encapsulated Core-shell up-conversion Nanoparticle Based Lateral Flow Strip Assay," *Talanta* 230 (2021): 122335, https://doi.org/10.1016/j.talanta.2021.122335.

15. L. Zhu, W. Fu, J. Chen, et al., "A Fully Integrated and Handheld Electrochemiluminescence Device for Detection of Dopamine in Biosamples," *Sensors and Actuators B: Chemical* 366 (2022): 131972, https://doi.org/10.1016/j.snb.2022.131972.

16. Y. Cui, S. Zhang, X. Zhou, F. Yan, and W. Hu, "Silica Nanochannel Array on Co-Electrodeposited Graphene-Carbon Nanotubes 3D Composite Film for Antifouling Detection of Uric Acid in Human Serum and Urine Samples," *Microchemical Journal* 190 (2023): 108632, https://doi.org/10.1016/j.microc.2023.108632.

17. K. Ma, L. Yang, J. Liu, and J. Liu, "Electrochemical Sensor Nanoarchitectonics for Sensitive Detection of Uric Acid in Human Whole Blood Based on Screen-Printed Carbon Electrode Equipped With Vertically-Ordered Mesoporous Silica-Nanochannel Film," *Nanomaterials* 12 (2022): 1157, https://doi.org/10.3390/nano12071157.

18. J. Wang, Z. Hou, W. Wang, et al., "Design of Self-Healing Nanocomposite Hydrogels and the Application to the Detection of Human Exercise and Ascorbic Acid in Sweat," *Biosensors and Bioelectronics* 267 (2025): 116767, https://doi.org/10.1016/j.bios.2024.116767.

19. W. Ling, X. Shang, J. Liu, and T. Tang, "A Skin-mountable Flexible Biosensor Based on Cu-MOF/PEDOT Composites for Sweat Ascorbic Acid Monitoring," *Biosensors and Bioelectronics* 267 (2025): 116852, https://doi.org/10.1016/j.bios.2024.116852.

20. J. Ding, X. Li, L. Zhou, R. Yang, F. Yan, and B. Su, "Electrodeposition of Nickel Nanostructures Using Silica Nanochannels as Confinement for Low-fouling Enzyme-free Glucose Detection," *Journal of Materials Chemistry B* 8 (2020): 3616–3622, https://doi.org/10.1039/C9TB02472G.

21. J. Huang, S. Xu, F. Yan, and J. Liu, "Electrochemiluminescence Enzyme Biosensors for Ultrasensitive Determination of Glucose Using Glucose Dehydrogenase Immobilized on Vertical Silica Nanochannels," *Sensors and Actuators B: Chemical* 402 (2024): 135119, https://doi.org/10.1016/j.snb.2023.135119.

22. Y. Luan, Y. Zhou, C. Li, et al., "Wearable Sensing Device Integrated With Prestored Reagents for Cortisol Detection in Sweat," *ACS Sensors* 9 (2024): 2075–2082, https://doi.org/10.1021/acssensors.4c00112.

23. R. Gupta, P. Singh, V. Ganesan, et al., "Palladium Nanoparticles Supported on Mesoporous Silica Microspheres for Enzyme-free Amperometric Detection of H2O2 Released From Living Cells," *Sensors and Actuators B: Chemical* 276 (2018): 517–525, https://doi.org/10.1016/j.snb.2018.08.148.

24. S. Ahoulou, N. Vilà, S. Pillet, D. Schaniel, and A. Walcarius, "Non-Covalent Immobilization of Iron-Triazole (Fe(Htrz) 3) Molecular Mediator in Mesoporous Silica Films for the Electrochemical Detection of Hydrogen Peroxide," *Electroanalysis* 32 (2020): 690–697, https://doi.org/10.1002/elan.201900444.

25. Z.-M. Lyu, X.-L. Zhou, X.-N. Wang, P. Li, L. Xu, and E. H. Liu, "Miniaturized Electrochemiluminescent Biochip Prepared on Gold Nanoparticles-Loaded Mesoporous Silica Film for Visual Detection of Hydrogen Peroxide Released From Living Cells," *Sensors and Actuators B: Chemical* 284 (2019): 437–443, https://doi.org/10.1016/j.snb.2018.12.149.

26. A. Walcarius, "Recent Trends on Electrochemical Sensors Based on Ordered Mesoporous Carbon," *Sensors* 17, no. 8 (2017): 1863, https://doi.org/10.3390/s17081863.

27. M. Etienne, L. Zhang, N. Vilà, and A. Walcarius, "Mesoporous Materials-Based Electrochemical Enzymatic Biosensors," *Electroanalysis* 27 (2015): 2028–2054, https://doi.org/10.1002/elan.201500172.

28. M. L. Scala-Benuzzi, S. N. Fernández, G. Giménez, G. Ybarra, and G. J. A. A. Soler-Illia, "Ordered Mesoporous Electrodes for Sensing Applications," *ACS Omega* 8 (2023): 24128–24152, https://doi.org/10.1021/acsomega.3c02013.

29. J. Bashir, M. B. Chowdhury, R. R. Kathak, et al., "Electrochemical Fabrication of Mesoporous Metal-Alloy Films," *Materials Advances* 4 (2023): 408–431, https://doi.org/10.1039/D2MA00480A.

30. F. Yan, X. Lin, and B. Su, "Vertically Ordered Silica Mesochannel Films: Electrochemistry and Analytical Applications," *The Analyst* 141 (2016): 3482–3495, https://doi.org/10.1039/C6AN00146G.

31. P. Zhou, L. Yao, K. Chen, and B. Su, "Silica Nanochannel Membranes for Electrochemical Analysis and Molecular Sieving: A Comprehensive Review," *Critical Reviews in Analytical Chemistry* 50 (2020): 424–444, https://doi.org/10.1080/10408347.2019.1642735.

32. M. Hasanzadeh, N. Shadjou, M. de la Guardia, M. Eskandani, and P. Sheikhzadeh, "Mesoporous Silica-Based Materials for Use in Biosensors," *TrAC Trends in Analytical Chemistry* 33 (2012): 117–129, https://doi.org/10.1016/j.trac.2011.10.011.

33. S. Li, H. Zhang, M. Zhu, et al., "Electrochemical Biosensors for Whole Blood Analysis: Recent Progress, Challenges, and Future Perspectives," *Chemical Reviews* 123, no. 12 (2023): 7953–8039, https://doi.org/10.1021/acs.chemrev.1c00759.

34. D. Grieshaber, R. MacKenzie, J. Vörös, and E. Reimhult, "Electrochemical Biosensors—Sensor Principles and Architectures," *Sensors* 8 (2008): 1400–1458, https://doi.org/10.3390/s80314000.

35. I.-H. Cho, D. H. Kim, and S. Park, "Electrochemical Biosensors: Perspective on Functional Nanomaterials for On-Site Analysis," *Biomaterials Research* 24, no. 1 (2020): 6, https://doi.org/10.1186/s40824-019-0181-y.

36. M. M. Shanbhag, G. Manasa, R. J. Mascarenhas, K. Mondal, and N. P. Shetti, "Fundamentals of Bio-Electrochemical Sensing," *Chemical Engineering Journal Advances* 16 (2023): 100516, https://doi.org/10.1016/j.ceja.2023.100516.

37. O. Tananaiko and A. Walcarius, "Composite Silica-Based Films as Platforms for Electrochemical Sensors," *The Chemical Record* 24, no. 2 (2024): 202300194, https://doi.org/10.1002/tcr.202300194.

38. G. Collins, P. R. Kasturi, R. Karthik, J.-J. Shim, R. Sukanya, and C. B. Breslin, "Mesoporous Carbon-Based Materials and Their Applications as Non-Precious Metal Electrocatalysts in the Oxygen Reduction Reaction," *Electrochimica Acta* 439 (2023): 141678, https://doi.org/10.1016/j.electacta.2022.141678.

39. X. Yang, P. Qiu, J. Yang, et al., "Mesoporous Materials–Based Electrochemical Biosensors From Enzymatic to Nonenzymatic," *Small* 17, no. 9 (2021): 1904022, https://doi.org/10.1002/smll.201904022.

40. Z. Li, L. Liu, Z. Wang, P. Gao, and G. K. Li, "Synthesis and Application of Mesoporous Materials: Process Status, Technical Problems, and Development Prospects: A Mini-Review," *Energy & Fuels* 37, no. 5 (2023): 3413–3427, https://doi.org/10.1021/acs.energyfuels.2c03882.

41. B. Xu, S. Li, R. Shi, and H. Liu, "Multifunctional Mesoporous Silica Nanoparticles for Biomedical Applications," *Signal Transduction and Targeted Therapy* 8 (2023): 435, https://doi.org/10.1038/s41392-023-01654-7.

42. K. Lan and D. Zhao, "Functional Ordered Mesoporous Materials: Present and Future," *Nano Letters* 22 (2022): 3177–3179, https://doi.org/10.1021/acs.nanolett.2c00902.

43. S. L. Suib, "A Review of Recent Developments of Mesoporous Materials," *The Chemical Record* 17 (2017): 1169–1183, https://doi.org/10.1002/tcr.201700025.

44. S. Kausar, M. Yousaf, S. Mir, N. S. Awwad, H. A. Alturaifi, and F. Riaz, "Mesoporous Materials: Synthesis and Electrochemical Applications,"

Electrochemistry Communications 169 (2024): 107836, https://doi.org/10.1016/j.elecom.2024.107836.

45. S. Mehdipour-Ataei and E. Aram, "Mesoporous Carbon-Based Materials: A Review of Synthesis, Modification, and Applications," *Catalysts* 13, no. 1 (2023): 2, https://doi.org/10.3390/catal13010002.

46. M. Ghaferi, K. M. E. Maedeh, R. Aun, A. H. Sitah, E. S. Hasan, and S. E. Alavi, "Mesoporous Silica Nanoparticles: Synthesis Methods and Their Therapeutic Use-recent Advances," *Journal of Drug Targeting* 29 (2021): 131–154, https://doi.org/10.1080/1061186X.2020.1812614.

47. J. A. S. Costa, R. A. de Jesus, D. O. Santos, J. B. Neris, R. T. Figueiredo, and C. M. Paranhos, "Synthesis, Functionalization, and Environmental Application of Silica-based Mesoporous Materials of the M41S and SBA-n Families: A Review," *Journal of Environmental Chemical Engineering* 9 (2021): 105259, https://doi.org/10.1016/j.jece.2021.105259.

48. M. R. Abukhadra, N. M. Refay, A. M. El-Sherbeeny, and M. A. El-Meligy, "Insight Into the Loading and Release Properties of MCM-48/Biopolymer Composites as Carriers for 5-Fluorouracil: Equilibrium Modeling and Pharmacokinetic Studies," *ACS Omega* 5 (2020): 11745–11755, https://doi.org/10.1021/acsomega.0c01078.

49. A. Yousefi and A. Babaei, "A New Sensor Based on Glassy Carbon Electrode Modified With Fe3O4@MCM-48-SO3H/Multi-wall Carbon Nanotubes Composite for Simultaneous Determination of Norepinephrine and Tyrosine in the Presence of Ascorbic Acid," *Ionics* 25 (2019): 2845–2856, https://doi.org/10.1007/s11581-018-2815-9.

50. M. Ghalkhani and E. Sohouli, "Synthesis of the Decorated Carbon Nano Onions With Aminated MCM-41/Fe3O4 NPs: Morphology and Electrochemical Sensing Performance for Methotrexate Analysis," *Microporous and Mesoporous Materials* 331 (2022): 111658, https://doi.org/10.1016/j.micromeso.2021.111658.

51. O. S. Tkachenko, L. V. Souza, M. Deon, et al., "AgNP-decorated SBA-15 for MWCNT Paste Modified Electrode: A Sensor for Simultaneous Voltammetric Determination of Paracetamol and Sulfamethoxazole," *Electroanalysis* 33 (2021): 29–37, https://doi.org/10.1002/elan.202060090.

52. X. Bai, X. Li, S. Li, et al., "A Stable Au–N Bond Controlled Probe Immobilization Approach for the Sensitive Detection Of Kirsten Rat Sarcoma Viral Oncogene DNA Using NH2-HMS@Au," *Journal of Materials Science* 57 (2022): 10328–10342, https://doi.org/10.1007/s10853-022-07314-5.

53. B. Karimi, N. Ganji, O. Pourshiani, and W. R. Thiel, "Periodic Mesoporous Organosilicas (PMOs): From Synthesis Strategies to Applications," *Progress in Materials Science* 125 (2022): 100896, https://doi.org/10.1016/j.pmatsci.2021.100896.

54. K. K. Maurya, K. Singh, and M. Malviya, "Effect of Palladium and Its Nanogeometry on the Redox Electrochemistry of Tetracyanoquinodimethane Modified Electrode; Application in Electrochemical Sensing of Ascorbic Acid," *Journal of Applied Electrochemistry* 53 (2023): 1831–1842, https://doi.org/10.1007/s10800-023-01878-z.

55. L. Morillas-Becerril, E. Peta, L. Gabrielli, et al., "Multifunctional, CD44v6-Targeted ORMOSIL Nanoparticles Enhance Drugs Toxicity in Cancer Cells," *Nanomaterials* 10 (2020): 298, https://doi.org/10.3390/nano10020298.

56. S. Shirazian, N. Pirestani, A. E. G. Baker, and R. Soltani, "A Comprehensive Review of KCC-1 Fibrous Silica for Water Treatment," *npj Clean Water* 8, no. 1 (2025): 3, https://doi.org/10.1038/s41545-025-00435-9.

57. W. Yang, S. Shirazian, R. Soltani, and M. H. Zare, "Bio-originated Mesosilicate SBA-15: Synthesis, Characterization, and Application for Heavy Metal Removal," *npj Clean Water* 7, no. 1 (2024): 49, https://doi.org/10.1038/s41545-024-00340-7.

58. M. Manzano and M. Vallet-Regí, "Mesoporous Silica Nanoparticles for Drug Delivery," *Advanced Functional Materials* 30, no. 2 (2020): 1902634, https://doi.org/10.1002/adfm.201902634.

59. B. Escriche-Navarro, A. Escudero, E. Lucena-Sánchez, F. Sancenón, A. García-Fernández, and R. Martínez-Máñez, "Mesoporous Silica Materials as an Emerging Tool for Cancer Immunotherapy," *Advanced Science* 9, no. 26 (2022): 2200756, https://doi.org/10.1002/advs.202200756.

60. M. J. Mitchell, M. M. Billingsley, R. M. Haley, M. E. Wechsler, N. A. Peppas, and R. Langer, "Engineering Precision Nanoparticles for Drug Delivery," *Nature Reviews Drug Discovery* 20 (2021): 101–124, https://doi.org/10.1038/s41573-020-0090-8.

61. S. Jafari, H. Derakhshankhah, L. Alaei, A. Fattahi, B. S. Varnamkhasti, and A. A. Saboury, "Mesoporous Silica Nanoparticles for Therapeutic/Diagnostic Applications," *Biomedicine & Pharmacotherapy* 109 (2019): 1100–1111, https://doi.org/10.1016/j.biopha.2018.10.167.

62. M. M. Abeer, P. Rewatkar, Z. Qu, et al., "Silica Nanoparticles: A Promising Platform for Enhanced Oral Delivery of Macromolecules," *Journal of Controlled Release* 326 (2020): 544–555, https://doi.org/10.1016/j.jconrel.2020.07.021.

63. S. Varshney, N. J. P. S. Abhishek, and N. Mishra, "An Overview on Biomedical Applications of Versatile Silica Nanoparticles, Synthesized via Several Chemical and Biological Routes: A Review," *Phosphorus, Sulfur, and Silicon and the Related Elements* 197 (2022): 72–88, https://doi.org/10.1080/10426507.2021.2017434.

64. S. Jimenez-Falcao, J. Parra-Nieto, H. Pérez-Cuadrado, R. Martínez-Máñez, P. Martínez-Ruiz, and R. Villalonga, "Avidin-Gated Mesoporous Silica Nanoparticles for Signal Amplification in Electrochemical Biosensor," *Electrochemistry Communications* 108 (2019): 106556, https://doi.org/10.1016/j.elecom.2019.106556.

65. B. Li, Y. Li, C. Li, et al., "An Ultrasensitive Split-type Electrochemical Immunosensor Based on Controlled-release Strategy for Detection of CA19-9," *Biosensors and Bioelectronics* 227 (2023): 115180, https://doi.org/10.1016/j.bios.2023.115180.

66. M. Rahal, C. Karman, N. Vilà, et al., "Vertically Aligned Mesoporous Silica Films Bearing Covalently Bound Tris(2,2′-bipyridyl)Ruthenium(II) Redox Photocatalysts," *Microporous and Mesoporous Materials* 387 (2025): 113524, https://doi.org/10.1016/j.micromeso.2025.113524.

67. J. Liu, D. He, Q. Liu, et al., "Vertically Ordered Mesoporous Silica Film-Assisted Label-Free and Universal Electrochemiluminescence Aptasensor Platform," *Analytical Chemistry* 88 (2016): 11707–11713, https://doi.org/10.1021/acs.analchem.6b03317.

68. F. Yan, T. Luo, Q. Jin, et al., "Tailoring Molecular Permeability of Vertically-ordered Mesoporous Silica-nanochannel Films on Graphene for Selectively Enhanced Determination of Dihydroxybenzene Isomers in Environmental Water Samples," *Journal of Hazardous Materials* 410 (2021): 124636, https://doi.org/10.1016/j.jhazmat.2020.124636.

69. G. Zhu, W. Bao, M. Xie, et al., "Accelerating Tandem Electroreduction of Nitrate to Ammonia via Multi-Site Synergy in Mesoporous Carbon-Supported High-Entropy Intermetallics," *Advanced Materials* 37, no. 5 (2025): 2413560, https://doi.org/10.1002/adma.202413560.

70. G. Zhu, Y. Jiang, H. Yang, H. Wang, Y. Fang, L. Wang, M. Xie, P. Qiu, and W. Luo, "Constructing Structurally Ordered High-Entropy Alloy Nanoparticles on Nitrogen-Rich Mesoporous Carbon Nanosheets for High-Performance Oxygen Reduction," *Advanced Materials* 34, no. 15 (2022): 2110128, https://doi.org/10.1002/adma.202110128.

71. P. Barathi, B. Thirumalraj, S.-M. Chen, and S. Angaiah, "A Simple and Flexible Enzymatic Glucose Biosensor Using Chitosan Entrapped Mesoporous Carbon Nanocomposite," *Microchemical Journal* 147 (2019): 848–856, https://doi.org/10.1016/j.microc.2019.03.083.

72. Z. Liu, F. Zhong, Z. Wu, et al., "Disposable Electrochemical Aptasensor With Mesoporous Carbon Spheres Modified Screen-Printed Dual-Working Electrodes for Pb2+ and Hg2+ Detection," *Sensors and Actuators B: Chemical* 422 (2025): 136558, https://doi.org/10.1016/j.snb.2024.136558.

73. X. Zhong, F. Wang, J. Piao, and Y. Chen, "Fabrication and Application of a Novel Electrochemical Biosensor Based on a Mesoporous Carbon Sphere@UiO-66-NH2/Lac Complex Enzyme for Tetracycline Detection," *The Analyst* 146 (2021): 2825–2833, https://doi.org/10.1039/D0AN02430A.

74. L. Wang, X.-H. Shi, Y.-F. Zhang, et al., "CdZnSeS Quantum Dots Condensed With Ordered Mesoporous Carbon for High-Sensitive Electrochemiluminescence Detection of Hydrogen Peroxide in Live Cells,"

Electrochimica Acta 362 (2020): 137107, https://doi.org/10.1016/j.electacta.2020.137107.

75. P. Balasubramanian, T. S. T. Balamurugan, S.-M. Chen, T.-W. Chen, and P.-H. Lin, "A Novel, Efficient Electrochemical Sensor for the Detection of Isoniazid Based on the B/N Doped Mesoporous Carbon Modified Electrode," *Sensors and Actuators B: Chemical* 283 (2019): 613–620, https://doi.org/10.1016/j.snb.2018.12.020.

76. D. Dăscălescu and C. Apetrei, "Development of a Novel Electrochemical Biosensor Based on Organized Mesoporous Carbon and Laccase for the Detection of Serotonin in Food Supplements," *Chemosensors* 10 (2022): 365, https://doi.org/10.3390/chemosensors10090365.

77. R. Jain, V. Nirbhaya, R. Chandra, and S. Kumar, "Nanostructured Mesoporous Carbon Based Electrochemical Biosensor for Efficient Detection of Swine Flu," *Electroanalysis* 34 (2022): 43–55, https://doi.org/10.1002/elan.202100242.

78. M. D. A. Wahab, S. M. A. Hossain, M. K. Masud, et al., "Nanoarchitectured Superparamagnetic Iron Oxide-Doped Mesoporous Carbon Nanozymes for Glucose Sensing," *Sensors and Actuators B: Chemical* 366 (2022): 131980, https://doi.org/10.1016/j.snb.2022.131980.

79. M. Ni, L. Sun, and B. Liu, "Mesoporous Gold Nanostructures: Synthesis and Beyond," *The Journal of Physical Chemistry Letters* 13 (2022): 4410–4418, https://doi.org/10.1021/acs.jpclett.2c01092.

80. H. Lv, D. Xu, L. Sun, et al., "Asymmetric Multimetallic Mesoporous Nanospheres," *Nano Letters* 19 (2019): 3379–3385, https://doi.org/10.1021/acs.nanolett.9b01223.

81. S. Chatterjee, C. Griego, J. L. Hart, et al., "Free Standing Nanoporous Palladium Alloys as CO Poisoning Tolerant Electrocatalysts for the Electrochemical Reduction of CO2 to Formate," *ACS Catalysis* 9 (2019): 5290–5301, https://doi.org/10.1021/acscatal.9b00330.

82. H. Lv, D. Xu, L. Sun, et al., "Ternary Palladium–Boron–Phosphorus Alloy Mesoporous Nanospheres for Highly Efficient Electrocatalysis," *ACS Nano* 13 (2019): 12052–12061, https://doi.org/10.1021/acsnano.9b06339.

83. Y. Zhou, R. Zhou, X. Zhu, et al., "Mesoporous PdAg Nanospheres for Stable Electrochemical CO2 Reduction to Formate," *Advanced Materials* 32, no. 30 (2020): 2000992, https://doi.org/10.1002/adma.202000992.

84. H. Lv, H. Qin, M. Sun, F. Jia, B. Huang, and B. Liu, "Mesoporosity-Enabled Selectivity of Mesoporous Palladium-Based Nanocrystals Catalysts in Semihydrogenation of Alkynes," *Angewandte Chemie International Edition* 61, no. 8 (2022): 202114539, https://doi.org/10.1002/anie.202114539.

85. Y. Feng, C.-Q. Cheng, C.-Q. Zou, et al., "Electroreduction of Carbon Dioxide in Metallic Nanopores Through a Pincer Mechanism," *Angewandte Chemie International Edition* 59 (2020): 19297–19303, https://doi.org/10.1002/anie.202008852.

86. H. Lv, H. Qin, K. Ariga, Y. Yamauchi, and B. Liu, "A General Concurrent Template Strategy for Ordered Mesoporous Intermetallic Nanoparticles With Controllable Catalytic Performance," *Angewandte Chemie International Edition* 61, no. 17 (2022): 202116179, https://doi.org/10.1002/anie.202116179.

87. E. Ahmed, M. K. Masud, M. S. A. Hossain, et al., "Nanostructured Mesoporous Gold Electrodes Detect Protein Phosphorylation in Cancer With Electrochemical Signal Amplification," *The Analyst* 145 (2020): 6639–6648, https://doi.org/10.1039/D0AN01096K.

88. E. Ahmed, M. K. Masud, P. Komatineni, et al., "A Mesoporous Gold Biosensor to Investigate Immune Checkpoint Protein Heterogeneity in Single Lung Cancer Cells," *Biosensors and Bioelectronics* 249 (2024): 115984, https://doi.org/10.1016/j.bios.2023.115984.

89. M. K. Masud, J. Na, T.-E. N. Lin, et al., "Nanostructured Mesoporous Gold Biosensor for microRNA Detection at Attomolar Level," *Biosensors and Bioelectronics* 168 (2020): 112429, https://doi.org/10.1016/j.bios.2020.112429.

90. H. Park, M. K. Masud, A. Ashok, et al., "Mesoporous Gold: Substrate-Dependent Growth Dynamics, Strain Accumulation, and Electrocatalytic Activity for Biosensing," *Small* 20, no. 35 (2024): 2311645, https://doi.org/10.1002/smll.202311645.

91. A. S. Nugraha, G. Lambard, J. Na, et al., "Mesoporous Trimetallic PtPdAu Alloy Films Toward Enhanced Electrocatalytic Activity in Methanol Oxidation: Unexpected Chemical Compositions Discovered by Bayesian Optimization," *Journal of Materials Chemistry A* 8 (2020): 13532–13540, https://doi.org/10.1039/D0TA04096G.

92. X. Gao, X. Pei, D. W. Gardner, et al., "Casting Nanoporous Platinum in Metal–Organic Frameworks," *Advanced Materials* 31, no. 12 (2019): 1807553, https://doi.org/10.1002/adma.201807553.

93. K.-H. Huynh, X.-H. Pham, J. Kim, et al., "Synthesis, Properties, and Biological Applications of Metallic Alloy Nanoparticles," *International Journal of Molecular Sciences* 21 (2020): 5174, https://doi.org/10.3390/ijms21145174.

94. K. Kani, H. Lim, A. E. Whitten, et al., "First Electrochemical Synthesis of Mesoporous RhNi Alloy Films for an Alkali-mediated Hydrogen Evolution Reaction," *Journal of Materials Chemistry A* 9 (2021): 2754–2763, https://doi.org/10.1039/D0TA09348C.

95. H. Park, M. K. Masud, J. Na, et al., "Mesoporous Gold–Silver Alloy Films Towards Amplification-Free Ultra-Sensitive MicroRNA Detection," *Journal of Materials Chemistry B* 8 (2020): 9512–9523, https://doi.org/10.1039/D0TB02003F.

96. H. Lv, L. Sun, J. Feng, et al., "Plasmonic Mesoporous AuAg Nanospheres With Controllable Nanostructures," *Chemical Communications* 56 (2020): 9679–9682, https://doi.org/10.1039/D0CC02524K.

97. T. Nagaura, H.-P. Phan, V. Malgras, et al., "Universal Electrochemical Synthesis of Mesoporous Chalcogenide Semiconductors: Mesoporous CdSe and CdTe Thin Films for Optoelectronic Applications," *Angewandte Chemie International Edition* 60 (2021): 9660–9665, https://doi.org/10.1002/anie.202013541.

98. A. S. Nugraha, V. Malgras, M. Iqbal, et al., "Electrochemical Synthesis of Mesoporous Au–Cu Alloy Films With Vertically Oriented Mesochannels Using Block Copolymer Micelles," *ACS Applied Materials & Interfaces* 10 (2018): 23783–23791, https://doi.org/10.1021/acsami.8b05517.

99. A. S. Nugraha, J. Na, M. S. A. Hossain, et al., "Block Copolymer-templated Electrodeposition of Mesoporous Au-Ni Alloy Films With Tunable Composition," *Applied Materials Today* 18 (2020): 100526, https://doi.org/10.1016/j.apmt.2019.100526.

100. Y. Kang, M. K. Masud, Y. Guo, et al., "Au-Loaded Superparamagnetic Mesoporous Bimetallic CoFeB Nanovehicles for Sensitive Autoantibody Detection," *ACS Nano* 17 (2023): 3346–3357, https://doi.org/10.1021/acsnano.2c07694.

101. M. Li, P. Wang, F. Pei, et al., "A Novel Signal Amplification System Fabricated Immunosensor Based on Au Nanoparticles and Mesoporous Trimetallic PdPtCu Nanospheres for Sensitive Detection of Prostate Specific Antigen," *Sensors and Actuators B: Chemical* 261 (2018): 22–30, https://doi.org/10.1016/j.snb.2018.01.136.

102. F. Muench, L. Sun, T. Kottakkat, et al., "Free-Standing Networks of Core–Shell Metal and Metal Oxide Nanotubes for Glucose Sensing," *ACS Applied Materials & Interfaces* 9 (2017): 771–781, https://doi.org/10.1021/acsami.6b13979.

103. S. Tanaka, M. K. Masud, Y. V. Kaneti, et al., "Enhanced Peroxidase Mimetic Activity of Porous Iron Oxide Nanoflakes," *ChemNanoMat* 5 (2019): 506–513, https://doi.org/10.1002/cnma.201800487.

104. C. Xu, C. Lei, Y. Wang, and C. Yu, "Dendritic Mesoporous Nanoparticles: Structure, Synthesis and Properties," *Angewandte Chemie International Edition* 61, no. 12 (2022): 202112752, https://doi.org/10.1002/anie.202112752.

105. A. Li, X. Mu, T. Li, et al., "Formation of Porous Cu Hydroxy Double Salt Nanoflowers Derived From Metal-organic Frameworks With Efficient Peroxidase-Like Activity for Label-Free Detection of Glu-

cose," *Nanoscale* 10, no. 25 (2018): 11948–11954, https://doi.org/10.1039/c8nr02832j.

106. Z. Qin, Q. Cheng, Y. Lu, and J. Li, "Facile Synthesis of Hierarchically Mesoporous NiCo2O4 Nanowires for Sensitive Nonenzymatic Glucose Detection," *Applied Physics A* 123, no. 7 (2017): 492, https://doi.org/10.1007/s00339-017-1108-x.

107. D. Guo, Y. Fu, F. Bu, et al., "Monodisperse Ultrahigh Nitrogen-Containing Mesoporous Carbon Nanospheres From Melamine-Formaldehyde Resin," *Small Methods* 5, no. 5 (2021): 2001137, https://doi.org/10.1002/smtd.202001137.

108. H. Chen, C.-T. Hung, W. Zhang, et al., "Asymmetric Monolayer Mesoporous Nanosheets of Regularly Arranged Semi-Opened Pores via a Dual-Emulsion-Directed Micelle Assembly," *Journal of the American Chemical Society* 145 (2023): 27708–27717, https://doi.org/10.1021/jacs.3c09927.

109. J. G. Croissant, Y. Fatieiev, A. Almalik, and N. M. Khashab, "Mesoporous Silica and Organosilica Nanoparticles: Physical Chemistry, Biosafety, Delivery Strategies, and Biomedical Applications," *Advanced Healthcare Materials* 7, no. 4 (2018): 1700831, https://doi.org/10.1002/adhm.201700831.

110. D. Cheng, J. Zhang, J. Fu, H. Song, and C. Yu, "A Hierarchical Spatial Assembly Approach of Silica-polymer Composites Leads to Versatile Silica/Carbon Nanoparticles," *Science Advances* 9, no. 40 (2023): adi7502, https://doi.org/10.1126/sciadv.adi7502.

111. B. Jiang, C. Li, J. Tang, et al., "Tunable-Sized Polymeric Micelles and Their Assembly for the Preparation of Large Mesoporous Platinum Nanoparticles," *Angewandte Chemie International Edition* 55 (2016): 10037–10041, https://doi.org/10.1002/anie.201603967.

112. Y. Feng, P. Li, and J. Wei, "Engineering Functional Mesoporous Materials From Plant Polyphenol Based Coordination Polymers," *Coordination Chemistry Reviews* 468 (2022): 214649, https://doi.org/10.1016/j.ccr.2022.214649.

113. S. Tanaka, Y. V. Kaneti, R. Bhattacharjee, et al., "Mesoporous Iron Oxide Synthesized Using Poly(Styrene-b-Acrylic Acid-b-Ethylene Glycol) Block Copolymer Micelles as Templates for Colorimetric and Electrochemical Detection of Glucose," *ACS Applied Materials & Interfaces* 10 (2018): 1039–1049, https://doi.org/10.1021/acsami.7b13835.

114. M. K. Masud, J. Kim, M. D. M. Billah, et al., "Nanoarchitectured Peroxidase-mimetic Nanozymes: Mesoporous Nanocrystalline α- or γ-Iron Oxide?," *Journal of Materials Chemistry B* 7 (2019): 5412–5422, https://doi.org/10.1039/C9TB00989B.

115. X. Wang, J. Cui, S. Chen, Y. Yang, L. Gao, and Q. He, "Electrochemical Sensing of Pancreatic Cancer miR-1290 Based on Yeast-Templated Mesoporous TiO2 Modified Electrodes," *Analytica Chimica Acta* 1105 (2020): 82–86, https://doi.org/10.1016/j.aca.2020.01.030.

116. X. Chen and Q. Zhang, "Recent Advances in Mesoporous Metal-organic Frameworks," *Particuology* 45 (2019): 20–34, https://doi.org/10.1016/j.partic.2018.09.007.

117. D. Liu, D. Zou, H. Zhu, and J. Zhang, "Mesoporous Metal–Organic Frameworks: Synthetic Strategies and Emerging Applications," *Small* 14 (2018): 1801454, https://doi.org/10.1002/smll.201801454.

118. Y. Wu, J.-Y. Chen, and W.-M. He, "Surface-Enhanced Raman Spectroscopy Biosensor Based on Silver Nanoparticles@Metal-Organic Frameworks With Peroxidase-mimicking Activities for Ultrasensitive Monitoring of Blood Cholesterol," *Sensors and Actuators B: Chemical* 365 (2022): 131939, https://doi.org/10.1016/j.snb.2022.131939.

119. S. Liu, Y. Huo, S. Deng, et al., "A Facile Dual-Mode Aptasensor Based on AuNPs@MIL-101 Nanohybrids for Ultrasensitive Fluorescence and Surface-Enhanced Raman Spectroscopy Detection of Tetrodotoxin," *Biosensors and Bioelectronics* 201 (2022): 113891, https://doi.org/10.1016/j.bios.2021.113891.

120. X. Yin, L. Dou, H. Hu, et al., "An Immune-Scaffold Relying Biosensor for Simultaneous Detection of Nitrofurazone and Furazolidone," *Sensors and Actuators B: Chemical* 345 (2021): 130399, https://doi.org/10.1016/j.snb.2021.130399.

121. J. Fang, J. Li, R. Feng, et al., "Dual-quenching Electrochemiluminescence System Based on Novel Acceptor CoOOH@Au NPs for Early Detection of Procalcitonin," *Sensors and Actuators B: Chemical* 332 (2021): 129544, https://doi.org/10.1016/j.snb.2021.129544.

122. X. Wang, N. Gao, J. Zhao, G. Ling, and P. Zhang, "Applications of Material Institute Lavoisier (MIL) Based Materials as Nano Drug Delivery Carriers in Biomedicine," *Coordination Chemistry Reviews* 517 (2024): 216040, https://doi.org/10.1016/j.ccr.2024.216040.

123. S. Yang, X. Li, G. Zeng, et al., "Materials Institute Lavoisier (MIL) Based Materials for Photocatalytic Applications," *Coordination Chemistry Reviews* 438 (2021): 213874, https://doi.org/10.1016/j.ccr.2021.213874.

124. M. Lv, X. Cao, M. Tian, et al., "A Novel Electrochemical Biosensor Based on MIL-101-NH2 (Cr) Combining Target-Responsive Releasing and Self-Catalysis Strategy for p53 Detection," *Biosensors and Bioelectronics* 214 (2022): 114518, https://doi.org/10.1016/j.bios.2022.114518.

125. R. T. Massah, S. L. Zambou Jiokeng, J. Liang, et al., "Sensitive Electrochemical Sensor Based on an Aminated MIL-101(Cr) MOF for the Detection of Tartrazine," *ACS Omega* 7 (2022): 19420–19427, https://doi.org/10.1021/acsomega.2c01106.

126. M. Zou, M. Dong, and T. Zhao, "Advances in Metal-Organic Frameworks MIL-101(Cr)," *International Journal of Molecular Sciences* 23 (2022): 9396, https://doi.org/10.3390/ijms23169396.

127. A. P. Cote, A. I. Benin, N. W. Ockwig, M. O'Keeffe, A. J. Matzger, and O. M. Yaghi, "Porous, Crystalline, Covalent Organic Frameworks," *Science* 310, no. 5751 (2005): 1166–1170, https://doi.org/10.1126/science.1120411.

128. I. Nath, J. Chakraborty, K. S. Rawat, et al., "Mesoporous Acridinium-Based Covalent Organic Framework for Long-Lived Charge-Separated Exciton Mediated Photocatalytic [4+2] Annulation," *Advanced Materials* 37, no. 1 (2025): 2413060, https://doi.org/10.1002/adma.202413060.

129. L. Liao, X. Guan, H. Zheng, et al., "Three-dimensional Microporous and Mesoporous Covalent Organic Frameworks Based on Cubic Building Units," *Chemical Science* 13 (2022): 9305–9309, https://doi.org/10.1039/D2SC02365B.

130. L. Wang, H. Xie, Y. Lin, et al., "Covalent Organic Frameworks (COFs)-based Biosensors for the Assay of Disease Biomarkers With Clinical Applications," *Biosensors and Bioelectronics* 217 (2022): 114668, https://doi.org/10.1016/j.bios.2022.114668.

131. X. Fan, J. Wu, T. Zhang, and J. Liu, "Electrochemical/Electrochemiluminescence Sensors Based on Vertically-Ordered Mesoporous Silica Films for Biomedical Analytical Applications," *Chembiochem* 25, no. 21 (2024): 202400320, https://doi.org/10.1002/cbic.202400320.

132. B. Auer, S. G. Telfer, and A. J. Gross, "Metal Organic Frameworks for Bioelectrochemical Applications," *Electroanalysis* 35, no. 1 (2023): 202200145, https://doi.org/10.1002/elan.202200145.

133. T. Zhao, A. Elzatahry, X. Li, and D. Zhao, "Single-Micelle-Directed Synthesis of Mesoporous Materials," *Nature Reviews Materials* 4 (2019): 775–791, https://doi.org/10.1038/s41578-019-0144-x.

134. M. Dubey, S. Wadhwa, A. Mathur, and R. Kumar, "Progress in Mesoporous Ceria: A Review on Synthesis Strategies and Catalytic Applications," *Applied Surface Science Advances* 12 (2022): 100340, https://doi.org/10.1016/j.apsadv.2022.100340.

135. X. Lu, J. Wang, T. Li, et al., "N-Doped Hollow Carbon Nanoplates With Mesoporous Thin Shells towards High-performance Supercapacitors," *Journal of Power Sources* 542 (2022): 231776, https://doi.org/10.1016/j.jpowsour.2022.231776.

136. J. Han, H. Bao, J.-Q. Wang, et al., "3D N-Doped Ordered Mesoporous Carbon Supported Single-Atom Fe-N-C Catalysts With Superior Performance for Oxygen Reduction Reaction and Zinc-air Battery," *Applied*

Catalysis B: Environmental 280 (2021): 119411, https://doi.org/10.1016/j.apcatb.2020.119411.

137. P. Innocenzi, "Mesoporous Ordered Films via Self-assembly: Trends and Perspectives," *Chemical Science* 13 (2022): 13264–13279, https://doi.org/10.1039/D2SC04828K.

138. Z. Teng, G. Zheng, Y. Dou, et al., "Highly Ordered Mesoporous Silica Films With Perpendicular Mesochannels by a Simple Stöber-Solution Growth Approach," *Angewandte Chemie International Edition* 51 (2012): 2173–2177, https://doi.org/10.1002/anie.201108748.

139. A. Walcarius, "Electroinduced Surfactant Self-Assembly Driven to Vertical Growth of Oriented Mesoporous Films," *Accounts of Chemical Research* 54 (2021): 3563–3575, https://doi.org/10.1021/acs.accounts.1c00233.

140. A. Walcarius, E. Sibottier, M. Etienne, and J. Ghanbaja, "Electrochemically Assisted Self-assembly of Mesoporous Silica Thin Films," *Nature Materials* 6 (2007): 602–608, https://doi.org/10.1038/nmat1951.

141. S. L. Z. Jiokeng, I. K. Tonle, and A. Walcarius, "Amino-attapulgite/Mesoporous Silica Composite Films Generated by Electro-Assisted Self-Assembly for the Voltammetric Determination of Diclofenac," *Sensors and Actuators B: Chemical* 287 (2019): 296–305, https://doi.org/10.1016/j.snb.2019.02.038.

142. L. Huang, R. Su, and F. Xi, "Sensitive Detection of Noradrenaline in human Whole Blood Based on Au Nanoparticles Embedded Vertically-Ordered Silica Nanochannels Modified Pre-activated Glassy Carbon Electrodes," *Frontiers in Chemistry* 11 (2023), https://doi.org/10.3389/fchem.2023.1126213.

143. X. Jin, L. Gong, J. Liang, et al., "Polydopamine-Enhanced Vertically-Ordered Mesoporous Silica Film Anti-Fouling Electrochemical Aptasensor for Indicator-Free Vibrio Parahaemolyticus Discrimination Using Stable Inherent Au Signal," *Sensors and Actuators B: Chemical* 407 (2024): 135485, https://doi.org/10.1016/j.snb.2024.135485.

144. H. Li, G. Lu, Q. Dai, Y. Wang, Y. Guo, and Y. Guo, "Hierarchical Organization and Catalytic Activity of High-Surface-Area Mesoporous Ceria Microspheres Prepared via Hydrothermal Routes," *ACS Applied Materials & Interfaces* 2 (2010): 838–846, https://doi.org/10.1021/am900829y.

145. B. Siddiqui, A. U. Rehman, I.-U. Haq, A. A. Al-Dossary, A. Elaissari, and N. Ahmed, "Exploiting Recent Trends for the Synthesis and Surface Functionalization of Mesoporous Silica Nanoparticles towards Biomedical Applications," *International Journal of Pharmaceutics: X* 4 (2022): 100116, https://doi.org/10.1016/j.ijpx.2022.100116.

146. M. Benítez, C. Rodríguez-Carrillo, S. Sánchez-Artero, J. El Haskouri, P. Amorós, and J. V. Ros-Lis, "Scaled-Up Microwave-Assisted Batch and Flow Synthesis and Life Cycle Assessment of a Silica Mesoporous Material: UVM-7," *Green Chemistry* 26, no. 2 (2024): 785–793, https://doi.org/10.1039/D3GC02875E.

147. J. S. Abreu, L. M. Costa, L. D. L. Ferreira, et al., "Hydrothermal Treatment as a Tool to Tailor the Mesoporous Structure of Sol-Gel Silica," *Journal of Non-Crystalline Solids* 610 (2023): 122323, https://doi.org/10.1016/j.jnoncrysol.2023.122323.

148. S. Alberti, S. Schmidt, S. Hageneder, et al., "Large-Pore Mesoporous Silica: Template Design, Thin Film Preparation and Biomolecule Infiltration," *Materials Chemistry Frontiers* 7 (2023): 4142–4151, https://doi.org/10.1039/D3QM00378G.

149. Y. Qiu, A. Ashok, C. C. Nguyen, et al., "3D Mesoporous Electrodes Integrated With Soft Surgical Robotics for Putative Minimally Invasive Intraoperative Tumor Detection and Ablation Monitoring," *ACS Applied Materials & Interfaces* 17 (2025): 48440–48452, https://doi.org/10.1021/acsami.5c08891.

150. H. Zhou, X. Ma, A. Sailjoi, et al., "Vertical Silica Nanochannels Supported by Nanocarbon Composite for Simultaneous Detection of Serotonin and Melatonin in Biological Fluids," *Sensors and Actuators B: Chemical* 353 (2022): 131101, https://doi.org/10.1016/j.snb.2021.131101.

151. J. Zhou, Y. Zheng, and D. Chen, "Three-Dimensional Interconnected Porous Partially Unzipped MWCNT/Graphene Composite Aerogels as Electrodes for High-Performance Supercapacitors," *Nanomaterials* 12, no. 4 (2022): 620, https://doi.org/10.3390/nano12040620.

152. R. Liang, J. Jiang, Y. Zheng, et al., "Vertically Oriented Mesoporous Silica Film Modified Fluorine-Doped Tin Oxide Electrode for Enhanced Electrochemiluminescence Detection of Lidocaine in Serum," *RSC Advances* 11, no. 55 (2021): 34669–34675, https://doi.org/10.1039/D1RA06375H.

153. M. Zhang, Y. Zou, X. Zhou, F. Yan, and Z. Ding, "Vertically-Ordered Mesoporous Silica Films for Electrochemical Detection of Hg(II) Ion in Pharmaceuticals and Soil Samples," *Frontiers in Chemistry* 10 –2022 (2022), https://doi.org/10.3389/fchem.2022.952936.

154. D. P. Carroll and P. M. Mendes, "Recent Advances in Surface Modification and Antifouling Strategies for Electrochemical Sensing in Complex Biofluids," *Current Opinion in Electrochemistry* 40 (2023): 101319, https://doi.org/10.1016/j.coelec.2023.101319.

155. X. Li, L. Zhou, J. Ding, L. Sun, and B. Su, "Platinized Silica Nanoporous Membrane Electrodes for Low-Fouling Hydrogen Peroxide Detection," *ChemElectroChem* 7, no. 9 (2020): 2081–2086, https://doi.org/10.1002/celc.202000321.

156. L. Xuan, W. Liao, M. Wang, et al., "Integration of Vertically-ordered Mesoporous Silica-nanochannel Film With Electro-Activated Glassy Carbon Electrode for Improved Electroanalysis in Complex Samples," *Talanta* 225 (2021): 122066, https://doi.org/10.1016/j.talanta.2020.122066.

157. L. Zhou, H. Hou, H. Wei, et al., "In Vivo Monitoring of Oxygen in Rat Brain by Carbon Fiber Microelectrode Modified With Antifouling Nanoporous Membrane," *Analytical Chemistry* 91 (2019): 3645–3651, https://doi.org/10.1021/acs.analchem.8b05658.

158. A. G. Ochoa-Ruiz, G. Parra, D. López-Espinoza, et al., "Electrochemical Immunosensors: The Evolution From Elisa to EμPADs," *Electroanalysis* 35, no. 4 (2023): 202200053, https://doi.org/10.1002/elan.202200053.

159. K. Malecka-Baturo and I. Grabowska, "Efficiency of Electrochemical Immuno- vs. apta(geno)Sensors for Multiple Cancer Biomarkers Detection," *Talanta* 281 (2025): 126870, https://doi.org/10.1016/j.talanta.2024.126870.

160. B. Moussa, W. Kutner, T. Beduk, A. Sena-Torralba, and E. Mostafavi, "Electrochemical Bio- and Chemosensors for Cancer Biomarkers: Natural (With Antibodies) Versus Biomimicking Artificial (With aptamers and Molecularly Imprinted Polymers) Recognition," *Talanta* 267 (2024): 125259, https://doi.org/10.1016/j.talanta.2023.125259.

161. S. Arshavsky-Graham, C. Heuer, X. Jiang, and E. Segal, "Aptasensors Versus Immunosensors—Which Will Prevail?," *Engineering in Life Sciences* 22 (2022): 319–333, https://doi.org/10.1002/elsc.202100148.

162. M. Srivastava, N. R. Nirala, S. K. Srivastava, and R. Prakash, "A Comparative Study of Aptasensor Vs Immunosensor for Label-Free PSA Cancer Detection on GQDs-AuNRs Modified Screen-Printed Electrodes," *Scientific Reports* 8 (2018): 1923, https://doi.org/10.1038/s41598-018-19733-z.

163. F. Curti, S. Fortunati, W. Knoll, et al., "A Folding-Based Electrochemical Aptasensor for the Single-Step Detection of the SARS-CoV-2 Spike Protein," *ACS Applied Materials & Interfaces* 14 (2022): 19204–19211, https://doi.org/10.1021/acsami.2c02405.

164. K. Wang, X. Lin, X. Lv, et al., "Nanozyme-Based Aptasensors for the Detection of Tumor Biomarkers," *Journal of Biological Engineering* 19 (2025): 13, https://doi.org/10.1186/s13036-025-00485-0.

165. X. Mi, H. Li, R. Tan, and Y. Tu, "Dual-Modular Aptasensor for Detection of Cardiac Troponin I Based on Mesoporous Silica Films by Electrochemiluminescence/Electrochemical Impedance Spectroscopy," *Analytical Chemistry* 92 (2020): 14640–14647, https://doi.org/10.1021/acs.analchem.0c03130.

166. W. Argoubi, A. Sánchez, C. Parrado, N. Raouafi, and R. Villalonga, "Label-free Electrochemical Aptasensing Platform Based on Mesoporous Silica Thin Film for the Detection of Prostate Specific Antigen," *Sensors*

and Actuators B: Chemical 255 (2018): 309–315, https://doi.org/10.1016/j.snb.2017.08.045.

167. I. Lee, S.-E. Kim, J. Lee, et al., "A Self-calibrating Electrochemical Aptasensing Platform: Correcting External Interference Errors for the Reliable and Stable Detection of Avian Influenza Viruses," *Biosensors and Bioelectronics* 152 (2020): 112010, https://doi.org/10.1016/j.bios.2020.112010.

168. J. Driscoll, P. Gondaliya, D. A. Zinn, et al., "Using Aptamers for Targeted Delivery of RNA Therapies," *Molecular Therapy* 33 (2025): 1344–1367, https://doi.org/10.1016/j.ymthe.2025.02.047.

169. K. Ma, Y. Zheng, L. An, and J. Liu, "Ultrasensitive Immunosensor for Prostate-Specific Antigen Based on Enhanced Electrochemiluminescence by Vertically Ordered Mesoporous Silica-Nanochannel Film," *Frontiers in Chemistry* 10 (2022): 851178, https://doi.org/10.3389/fchem.2022.851178.

170. A. Tabrizi, M, and P. Acedo, "Highly Sensitive Aptasensor for the Detection of SARS-CoV-2-RBD Using Aptamer-gated Methylene Blue@Mesoporous Silica Film/Laser Engraved Graphene Electrode," *Biosensors and Bioelectronics* 215 (2022): 114556, https://doi.org/10.1016/j.bios.2022.114556.

171. J. Gong, T. Zhang, T. Luo, et al., "Bipolar Silica Nanochannel Array Confined Electrochemiluminescence for Ultrasensitive Detection of SARS-CoV-2 Antibody," *Biosensors and Bioelectronics* 215 (2022): 114563, https://doi.org/10.1016/j.bios.2022.114563.

172. J. Gong, T. Zhang, P. Chen, F. Yan, and J. Liu, "Bipolar Silica Nanochannel Array for Dual-mode Electrochemiluminescence and Electrochemical Immunosensing Platform," *Sensors and Actuators B: Chemical* 368 (2022): 132086, https://doi.org/10.1016/j.snb.2022.132086.

173. X. Zhou, Q. Han, J. Zhou, C. Liu, and J. Liu, "Reagentless Electrochemical Detection of Tumor Biomarker Based on Stable Confinement of Electrochemical Probe in Bipolar Silica Nanochannel Film," *Nanomaterials* 13 (2023): 1645, https://doi.org/10.3390/nano13101645.

174. J. Huang, T. Zhang, Y. Zheng, and J. Liu, "Dual-Mode Sensing Platform for Cancer Antigen 15-3 Determination Based on a Silica Nanochannel Array Using Electrochemiluminescence and Electrochemistry," *Biosensors* 13 (2023): 317, https://doi.org/10.3390/bios13030317.

175. Y. Wang, L. Ding, M. Du, et al., "Integrated Colorimetric Immunoassay for PSA Using Confined Pt Nanozymes and Smartphone-assisted Machine Learning Analysis," *Sensors and Actuators B: Chemical* 446 (2026): 138565, https://doi.org/10.1016/j.snb.2025.

Biographies

Vinh Khanh Ho is a Ph.D. candidate in Chemical Engineering at the Queensland Quantum and Advanced Technologies Research Institute, Griffith University, Australia under supervision of Prof. Nam-Trung Nguyen and Dr. Sina Jamali. He previously holds a B.Eng. Chemical Engineering (2021) and M.Eng. Chemical Engineering (2023) from Ho Chi Minh City University of Technology (HCMUT). His current research focuses on electrochemical wearable biosensors based on mesoporous materials for healthcare monitoring.

Dr Tuan-Khoa Nguyen's research spans engineering, physics, and micro/nanotechnology, with a particular emphasis on wide bandgap electronics for advanced sensing and bioelectronic applications. His program combines micro/nanotechnology, advanced manufacturing, and precision engineering to design and develop high-performance devices for physical sensing, wearable and implantable therapeutics, and ultrasensitive biosensing. Current projects investigate nanothin films for long-lived implanted devices, flexible electronic systems, and next-generation biosensing platforms addressing challenges in healthcare, biotechnology, and environmental monitoring. By advancing device innovation at the micro- and nanoscale, Dr Nguyen's work helps drive emerging technologies that bridge fundamental science with real-world practical applications.

Dr. Sina Jamali is an ARC DECRA Fellow and Senior Lecturer in the School of Environment and Science at Griffith University. He heads a research group working at the interface of electrochemistry, biointerfaces, and functional materials for next-generation diagnostics. He earned his Ph.D. from the University of Wollongong in 2016, followed by academic and industry roles and a DECRA Fellowship at UNSW Sydney before joining Griffith in 2024. His research centers around electroactive materials, stochastic electrochemical methods, and electroanalytical sensors, particularly for real-time monitoring, cell analysis, and POC devices.

Professor Nam-Trung Nguyen's research focuses on microfluidics, nanofluidics, micro/nanomachining technologies, micro/nanoscale science, and instrumentation for biomedical applications. He is a renowned leader in his field with over 680 research papers. He received his Dip-Ing, Dr Ing and Dr Ing Habil degrees from Chemnitz University of Technology, Germany, in 1993, 1997, and 2004, respectively. He is a Fellow of ASME and a Senior Member of IEEE. In 2012 he was a SMART Faculty Fellow, Singapore-MIT Alliance for Research and Technology. He is also an Elected Fellow of American Society of Mechanical Engineers and an Australian Research Council Laureate Fellow.